

## Table of Contents

1. Materials and Synthesis	2
2. Spectra: NMR & mass	6
3. Optical Spectra: Photoluminescence lifetimes, $g_{lum}$ -vs-wavelength	18
4. Computational studies	21
5. Cartesian Coordinates	34

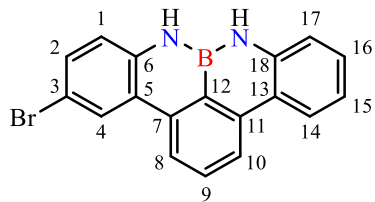
## 1. Materials and Synthesis

**General.** Unless otherwise indicated, all reactions were carried out under dry and inert conditions by heating all glassware with a heat gun under vacuum and purging with argon. All chemicals and solvents were purchased from commercial suppliers in anhydrous form or were dried by known methods or, in the case of THF were taken from a MBRAUN SPS 800 solvent purification system. Solvents were degassed by the freeze-pump-thaw method. TLC was done using precoated polyester sheets (40×80 mm) from Machery-Nagel (POLYGAM® SIL G/UV254) with 0.2 mm silica gel 60 with fluorescent indicator. A UV light source from Köhler (254 nm and 365 nm, 2·6 W) was used for visualization. NMR spectroscopy was done on Bruker Avance III 400, Bruker Avance III HDX 600, and Bruker Avance III HDX 700 spectrometers. Chemical shifts  $\delta$  are given in ppm, coupling constants  $J$  in hertz (Hz) and standard abbreviations are designated to the multiplicities of the signals. The spectra were calibrated with the solvent residual signals. High resolution mass spectrometry was done with electron spray ionization time of flight mass spectrometry (ESI-TOF-MS) on a maXis 4G Bruker system. UV/Vis absorption spectra were recorded on a PerkinElmer Lambda 1050 spectrometer with a PerkinElmer 3D WB Det Module in 1.0 cm quartz cuvettes, and samples were analyzed in CH<sub>2</sub>Cl<sub>2</sub> at room temperature. Steady-state excitation and emission spectra were recorded on a Horiba Fluorolog-3 DF spectrofluorimeter equipped with a 450 W Xe lamp, and samples were analysed in CH<sub>2</sub>Cl<sub>2</sub> at room temperature. Emission was monitored at a 90° angle using a Hamamatsu R2658P PMT (UV/Vis/NIR, 200 nm <  $\lambda_{\text{em}}$  < 1000 nm) detector. Spectral selection was achieved by the double grating monochromator 320DFX for excitation (1200 grooves/nm, blazed at 330 nm) and the single grating emission monochromator iHR550 for the visible path (1200 grooves/nm, blazed at 500 nm). For the lifetime measurements, a pulsed LED (Horiba DeltaDiode-310,  $\lambda_{\text{em}} = 308 \pm 10$  nm, pulse width ~1 ns FWHM, P<sub>avg</sub> = 5  $\mu$ W) was used. Lifetime data analysis (least square fitting, statistical parameters, etc.) was performed using the software package DAS from Horiba. Lifetimes were determined from the decay curves by an iterative deconvolution fitting method using appropriate multi-exponential functions and taking the instruments response function into account. The instrument used for determination of absolute fluorescence quantum yields was a PerkinElmer FL 8500 Spectrophotometer equipped with a 150 W continuous Xe short arc lamp as excitation source and an integration sphere. Quantum yields were averaged over 4 independent experiments. CPL measurements were carried out with a home-made spectrofluoropolarimeter,<sup>1</sup> mounting a Hamamatsu R-376. The samples concentration was around 2×10<sup>-6</sup> M in dichloromethane. A 365 nm LED was used as the excitation source, employing a 90° geometry. The excitation beam was horizontally polarized. Parameters: slit width = 5 nm, scan speed = 2 nm/sec, integration time = 2 sec, PMT voltage = 550 V, accumulations = 4. The solvent baseline was subtracted from the CPL spectra. ECD spectra were recorded with a Jasco J-1500 spectropolarimeter in dichloromethane solution. The spectra were baseline corrected. All measurements were done in spectroscopy grade solvents.

**Materials.** NBN-Benzo[f,g]tetracene (**3**)<sup>2</sup>, 1-bromo-3,9-dibutyl-NBN-benzo[f,g]tetracene (**5**)<sup>3,4</sup>, (*R*)-/(*S*)-3,3'-diiodo-2,2'-dimethoxy-1,1'-binaphthalene,<sup>5</sup> and (*R*)-/(*S*)-3,3'-diethynyl-2,2'-dimethoxy-1,1'-binaphthalene ((*R*)-/(*S*)-**6**)<sup>6</sup> were prepared according to literature procedures.

## Synthetic Procedures.

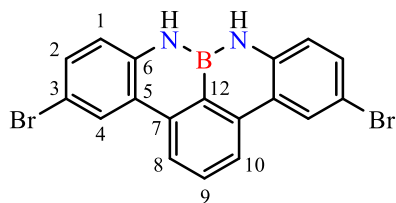
### 3-Bromo-NBN-benzo[*f,g*]tetracene (**4**)



Under ambient conditions, NBN-benzo[*f,g*]tetracene (697 mg, 2.60 mmol, 1.18 eq) is dissolved in acetonitrile (330 ml) and THF (40 ml). The solution is cooled to 0°C and a solution of NBS (393 mg, 2.21 mmol, 1.00 eq) in acetonitrile (20 ml) is added all at once. The cooling bath is not removed, but no additional ice is added so that the solution is allowed to slowly warm to r.t. over night. The mixture is concentrated under reduced pressure, redissolved in ethyl acetate (80 ml), and is transferred to a separation funnel. The organic phase is washed with saturated NaHCO<sub>3</sub> (80 ml), water (80 ml), and brine (50 ml), dried over MgSO<sub>4</sub> and is filtered. Silica is added and the solvent is removed under reduced pressure. The crude product is applied to silica gel chromatography (THF 2/5 hexanes, R<sub>f</sub> = 0.24 in THF 1/2 hexanes) and the product is obtained as a colourless solid (550 mg, 1.59 mmol, 72 %).

**<sup>1</sup>H NMR** (400 MHz, CD<sub>2</sub>Cl<sub>2</sub>): 8.34 (d, <sup>3</sup>J = 2.2 Hz, 1H, H-4), 8.24 (dd, <sup>3</sup>J = 8.1, <sup>4</sup>J = 1.5 Hz, 1H, H14), 8.21 (d, <sup>3</sup>J = 8.0 Hz, 1H, H10), 8.10 (d, <sup>3</sup>J = 8.0 Hz, 1H, H8), 7.82 (vt, <sup>3</sup>J = 8.0 Hz, 1H, H9), 7.39 (dd, <sup>3</sup>J = 8.5, <sup>4</sup>J = 2.2 Hz, 1H, H2), 7.36–7.31 (m, 1H, H16), 7.13–7.09 (m, 1H, H15), 7.09–7.06 (m, 1H, H17), 6.96 (d, <sup>3</sup>J = 8.5 Hz, 1H, H1), 6.49–6.36 (m, 2H, NH) ppm; **<sup>13</sup>C{<sup>1</sup>H} NMR** (101 MHz, CD<sub>2</sub>Cl<sub>2</sub>): δ 141.0 (C18), 140.3 (C6), 139.6 (C11), 138.3 (C7), 131.7 (C9), 131.5 (C2), 129.1 (C16), 127.6 (C4), 124.9 (C14), 124.7 (C5), 122.5 (C13), 120.7 (C15), 120.4 (C1), 120.2 (C10), 119.6 (C8), 118.9 (C17), 112.7 (C3) ppm; **<sup>11</sup>B{<sup>1</sup>H} NMR** (128 MHz, CD<sub>2</sub>Cl<sub>2</sub>): δ 26.8 ppm.

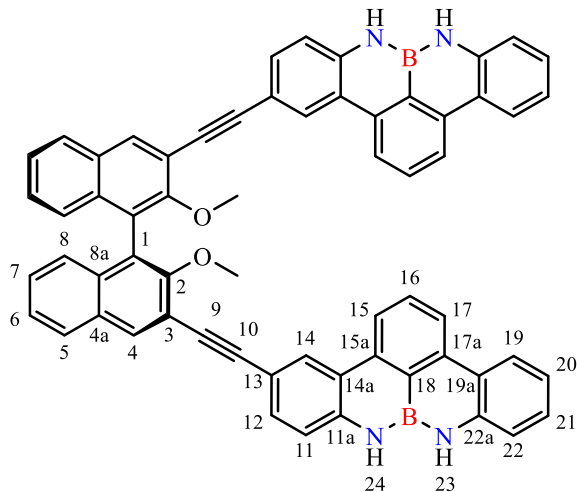
### 3,9-Dibromo-NBN-benzo[*f,g*]tetracene



Under ambient conditions, NBN-benzo[*f,g*]tetracene (500 mg, 1.86 mmol, 1.00 eq) is dissolved acetonitrile (270 ml) and THF (35 ml). NBS (663 mg, 3.73 mmol, 2.00 eq) is added at r.t. and the reaction mixture is stirred overnight. The solvent is removed under reduced pressure and the residue is suspended in acetonitrile (80 ml) and is treated with ultrasound for 5 min. Filtration and washing with acetonitrile (2×25 ml), water (2×25 ml), and MeOH (30 ml) yields the desired product as a colourless solid (500 mg, 1.17 mmol, 63 %).

**<sup>1</sup>H NMR** (400 MHz, THF-*d*<sub>8</sub>): δ 8.38 (d, <sup>4</sup>J = 2.2 Hz, 2H, H4), 8.21 (d, <sup>3</sup>J = 8.0 Hz, 2H, H8), 7.78 (t, <sup>3</sup>J = 8.0 Hz, 1H, H9), 7.35 (dd, <sup>3</sup>J = 8.6 Hz, <sup>4</sup>J = 2.2 Hz, 2H, H2), 7.05 (d, <sup>3</sup>J = 8.6 Hz, 2H, H1) ppm; **<sup>13</sup>C{<sup>1</sup>H} NMR** (101 MHz, THF-*d*<sub>8</sub>): δ 141.7 (C6), 139.1 (C7), 132.0 (C9), 131.8 (C2), 127.9 (C4), 128.4 (C10), 125.2 (C5), 121.0 (C1), 120.6 (C8), 112.8 (C3) ppm; **<sup>11</sup>B{<sup>1</sup>H} NMR** (128 MHz, CD<sub>2</sub>Cl<sub>2</sub>): δ 26.9 ppm.

**(R)-/(S)-3,3'-Bis(NBN-benzo[*f,g*]tetracen-3-yl-ethynyl)-2,2'-dimethoxy-1,1'-binaphthalene (1)**

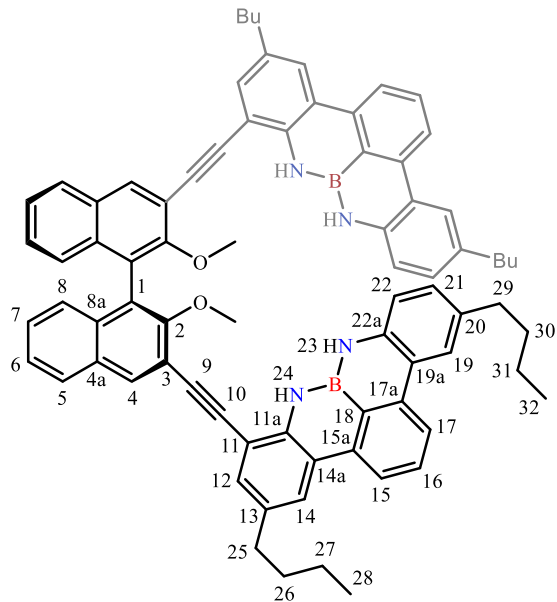


**(R)-6** (58.0 mg, 0.160 mmol, 1.00 eq), **1** (122 mg, 0.352 mmol, 2.20 eq),  $\text{Pd}_2(\text{dba})_3$  (10.3 mg, 11.2  $\mu\text{mol}$ , 0.07 eq),  $\text{CuI}$  (4.3 mg, 22.4  $\mu\text{mol}$ , 0.14 eq), and  $(t\text{-Bu})_3\text{PH}\times\text{BF}_4^-$  (13.0 mg, 44.8  $\mu\text{mol}$ , 0.28 eq) are suspended in dry, degassed  $\text{THF}/\text{Et}_3\text{N}$  (6 ml, 1/1 v/v). The reaction mixture is stirred at 55°C for 40 h. The mixture is allowed to cool to r.t. and the solvent is removed under reduced pressure. The complex product mixture is purified by a series of chromatographic methods. First, silica gel chromatography ( $\text{THF}$  2/1 hexane) is performed and the product fraction is applied to a recycling-GPC device using  $\text{THF}$  as eluent. The obtained two component fraction containing the product is separated by a final silica gel chromatography ( $\text{CH}_2\text{Cl}_2$  6/1 hexanes,  $R_f = 0.32$ ) yielding the product **(R)-1** as a pale yellow solid (59 mg, 66  $\mu\text{mol}$ , 41 %).  $[\alpha]_{589}^{20} - 349^\circ$  (c 0.10,  $\text{CHCl}_3$ ).

**(S)-1** is obtained by a similar procedure starting from **(S)-6**.  $[\alpha]_{589}^{20} + 354^\circ$  (c 0.10,  $\text{CHCl}_3$ ).

**$^1\text{H NMR}$**  (700 MHz,  $\text{CD}_2\text{Cl}_2$ ):  $\delta$  8.51 (d,  $^4J = 1.8$  Hz, 2H, H14), 8.30 (s, 2H, H4), 8.28 – 8.24 (m, 2H, H19), 8.22 (d,  $^3J = 8.0$  Hz, 4H, H15+ H17), 7.95 (d,  $^3J = 8.2$  Hz, 2H, H5), 7.84 (t,  $^3J = 8.0$  Hz, 2H, H16), 7.56 (dd,  $^3J = 8.3$ ,  $^4J = 1.8$  Hz, 2H, H12), 7.49 – 7.42 (m, 2H, H6), 7.37 – 7.32 (m, 2H, H21), 7.32 – 7.27 (m, 2H, H7), 7.20 – 7.14 (m, 2H, H8), 7.14 – 7.06 (m, 6H, H11+H20+H22), 6.53 (bs, 2H, NH), 6.48 (bs, 2H, NH), 3.84 (s, 6H, OMe) ppm;  **$^{13}\text{C}\{^1\text{H}\}$  NMR** (176 MHz,  $\text{CD}_2\text{Cl}_2$ ):  $\delta$  156.1 (C2), 141.8 (C11a), 141.0 (C22a), 139.6 (C17a), 138.7 (C15a), 134.3 (C4), 134.2 (C8a), 132.1 (C12), 131.8 (C16), 131.0 (C4a), 129.1 (C21), 128.5 (C14), 128.4 (C5), 127.6 (C7), 127.5 (C18), 126.2 (C8), 126.0 (C6), 125.6 (C1), 124.9 (C19), 123.0 (C14a), 122.7 (C19a), 120.7 (C20), 120.1 (C15), 119.7 (C17), 119.1 (C11), 118.9 (C22), 118.3 (C3), 115.0 (C13), 95.3 (C10), 85.4 (C9), 61.7 (OMe) ppm; **HRMS-ESI** calcd for  $\text{C}_{62}\text{H}_{40}\text{B}_2\text{N}_4\text{O}_2\text{Na}$   $[\text{M}+\text{Na}]^+$ : 917.32484, found: 917.32597 m/z.

**(R)-/(S)-3,3'-Bis(3,9-dibutyl-NBN-benzo[f,g]tetracen-1-yl-ethynyl)-2,2'-dimethoxy-1,1'-binaphthalene (2)**



**(R)-6** (58.0 mg, 0.160 mmol, 1.00 eq), **2** (162 mg, 0.352 mmol, 2.20 eq), Pd<sub>2</sub>(dba)<sub>3</sub> (10.3 mg, 11.2 µmol, 0.07 eq), CuI (4.3 mg, 22.4 µmol, 0.14 eq), and (t-Bu)<sub>3</sub>PH×BF<sub>4</sub> (13.0 mg, 44.8 µmol, 0.28 eq) are suspended in dry, degassed THF/Et<sub>3</sub>N (6 ml, 1/1 v/v). The reaction mixture is stirred at 55°C for 16 h. The mixture is allowed to cool to r.t. and the solvent is removed under reduced pressure. The complex product mixture is purified by a series of chromatographic methods. First, silica gel chromatography (THF/toluene/cyclohexane 1/34/65) is performed and the product fraction is applied to a recycling-GPC device (twice) using CHCl<sub>3</sub> as eluent. The product **(R)-2** is obtained as a yellow film (64 mg, 58 µmol, 36 %). [α]<sub>589</sub><sup>20</sup> – 328° (c 0.50, CHCl<sub>3</sub>).

**(S)-2** is obtained by a similar procedure starting from **(S)-6**. [α]<sub>589</sub><sup>20</sup> + 325° (c 0.50, CHCl<sub>3</sub>).

**<sup>1</sup>H NMR** (700 MHz, CD<sub>2</sub>Cl<sub>2</sub>): δ 8.40 (s, 2H, H4), 8.17 (d, <sup>3</sup>J = 8.0 Hz, 2H, H15), 8.14 (d, <sup>3</sup>J = 8.0 Hz, 2H, H17), 8.10 (d, <sup>4</sup>J = 1.9 Hz, 2H, H14), 8.03 (d, <sup>3</sup>J = 8.1 Hz, 2H, H5), 7.94 (d, <sup>4</sup>J = 1.8 Hz, 2H, H19), 7.86 (s, 2H, NH24), 7.79 (vt, <sup>3</sup>J = 8.0 Hz, 2H, H16), 7.59 – 7.51 (m, 2H, H6), 7.50 (d, <sup>4</sup>J = 1.9 Hz, 2H, H12), 7.42 – 7.35 (m, 2H, H7), 7.32 – 7.27 (m, 2H, H8), 6.94 (dd, <sup>3</sup>J = 8.1, <sup>4</sup>J = 1.8 Hz, 2H, H21), 6.84 (d, <sup>3</sup>J = 8.1 Hz, 2H, H22), 6.36 (s, 2H, NH23), 3.78 (s, 6H, OMe), 2.79 – 2.69 (m, 4H, H25), 2.62 – 2.54 (m, 4H, H29), 1.78 – 1.65 (m, 4H, H26), 1.60 – 1.50 (m, 4H, H30), 1.50 – 1.39 (m, 4H, H27), 1.39 – 1.29 (m, 4H, H31), 1.01 – 0.96 (m, 6H, H28), 0.94 – 0.89 (m, 6H, H32) ppm; **<sup>13</sup>C{<sup>1</sup>H} NMR** (176 MHz, CD<sub>2</sub>Cl<sub>2</sub>): δ 156.3 (C2), 141.0 (C11a), 139.7 (C17a), 139.2 (C15a), 138.9 (C22a), 134.8 (C20), 134.4 (C8a), 134.1 (C4), 134.0 (C13), 131.4 (C16), 131.2 (C12), 131.2 (C4a), 129.3 (C21), 128.7 (C5), 128.1 (C7), 127.7 (C18), 126.4 (C6+C8), 125.9 (C14), 125.5 (C1), 124.2 (C19), 122.6 (C14a), 122.2 (C19a), 119.6 (C15), 119.4 (C17), 118.8 (C22), 118.0 (C3), 111.5 (C11), 93.3 (C9), 91.9 (C10), 62.0 (OMe), 35.8 (C29), 35.7 (C25), 34.7 (C30), 34.6 (C26), 22.9 (C27+C31), 14.4 (C32), 14.3 (C28) ppm; **HRMS-ESI** calcd for C<sub>78</sub>H<sub>73</sub>B<sub>2</sub>N<sub>4</sub>O<sub>2</sub> [M+H]<sup>+</sup>: 1119.59367, found: 1119.59472 m/z.

## 2. Spectra: NMR & mass

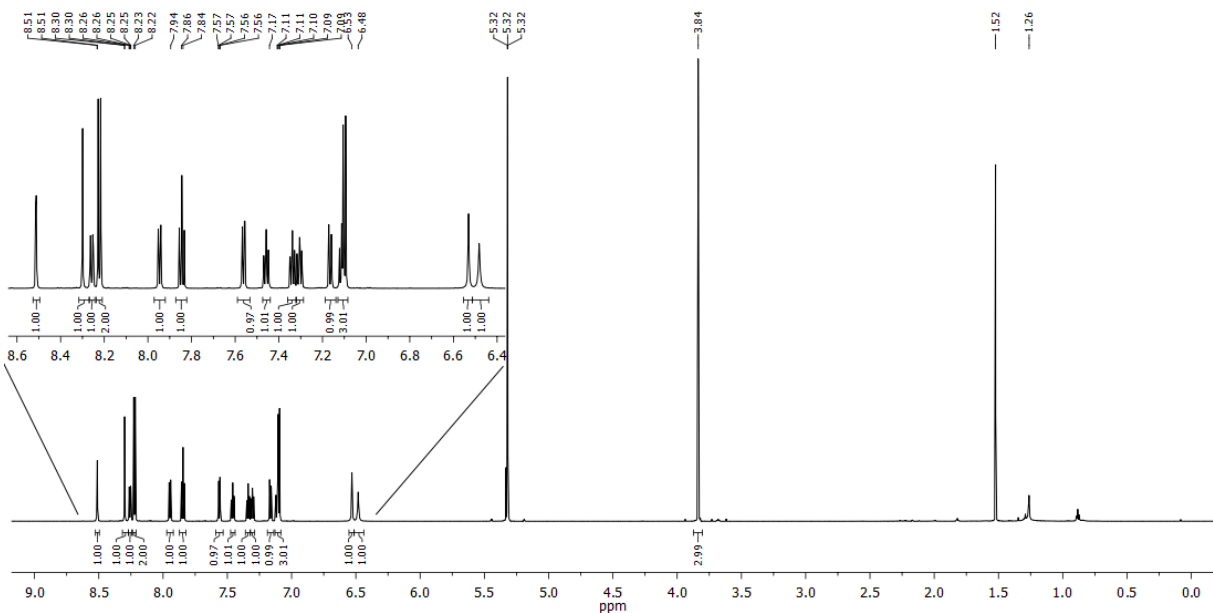


**Figure S1.**  $^1\text{H}$  NMR (700 MHz,  $\text{CD}_2\text{Cl}_2$ ) of (*S*)-1.

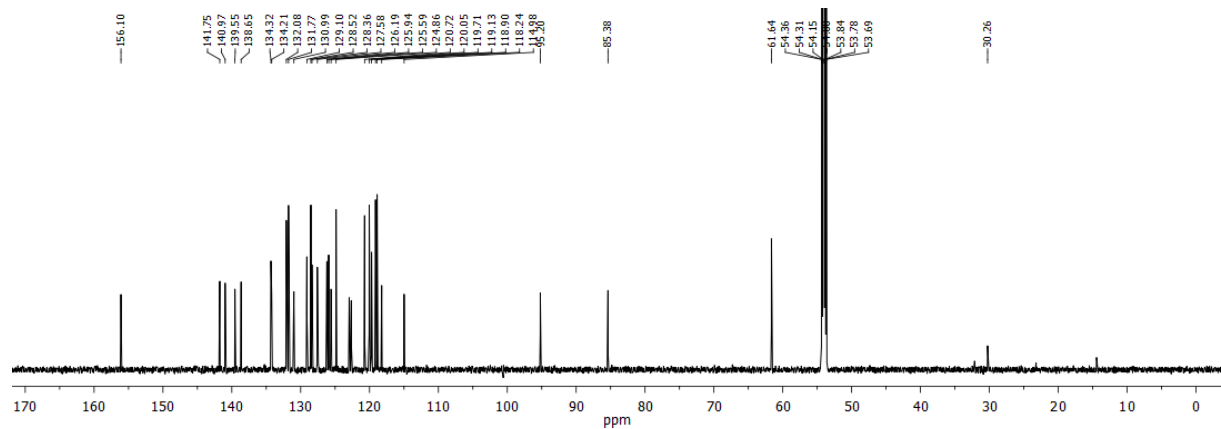


**Figure S2.**  $^{13}\text{C}\{^1\text{H}\}$  NMR (176 MHz,  $\text{CD}_2\text{Cl}_2$ ) of (*S*)-**1**.

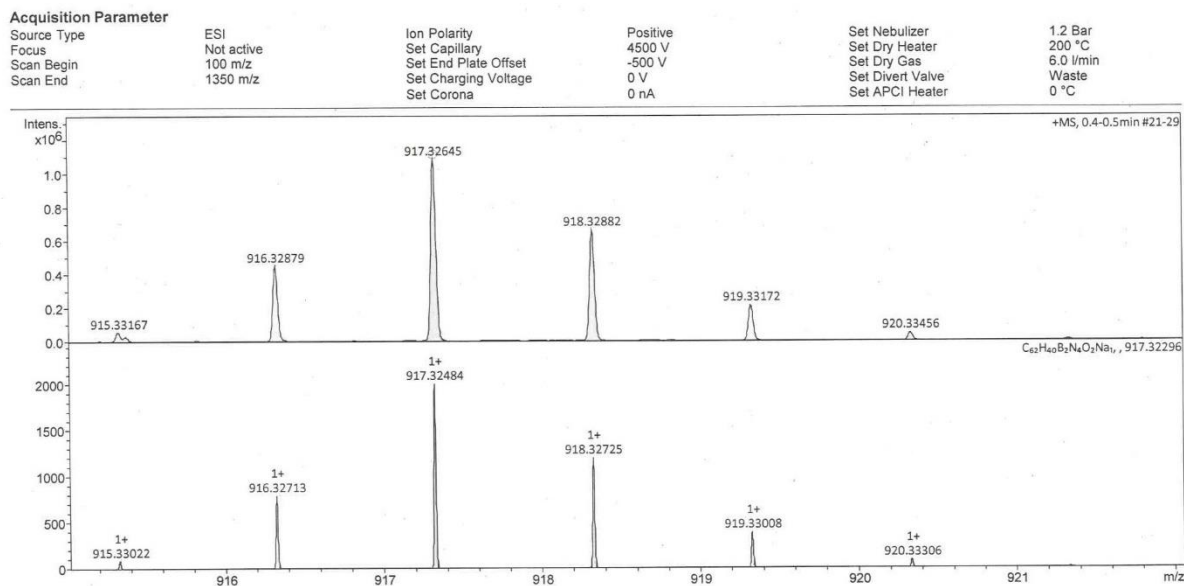


**Figure S3.** Experimental HR ESI-MS of (*S*)-1 (top) and theoretical isotopic envelopes for  $C_{62}H_{40}B_2N_4O_2Na$   $[M+Na]^+$  (bottom).  $m/z$   $[M+Na]^+$  calculated for  $C_{62}H_{40}B_2N_4O_2Na$ : 917.32484; found: 917.32645 ( $\Delta$ : 1.76 ppm).

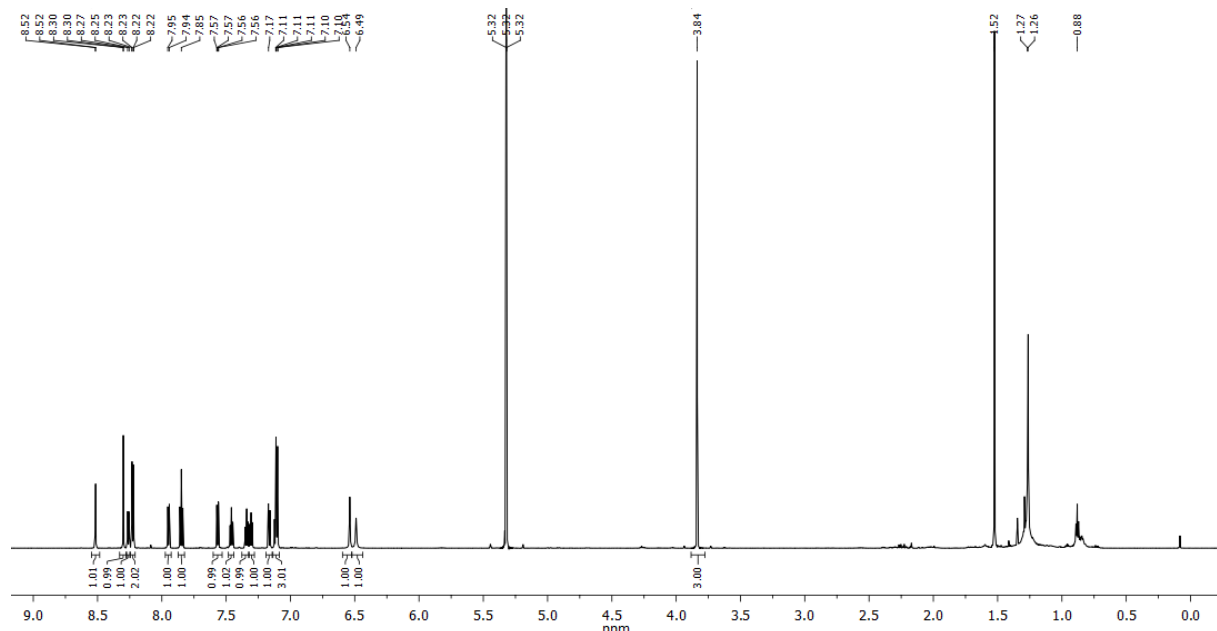


**Figure S4.**  $^1H$  NMR (700 MHz,  $CD_2Cl_2$ ) of (*R*)-1.

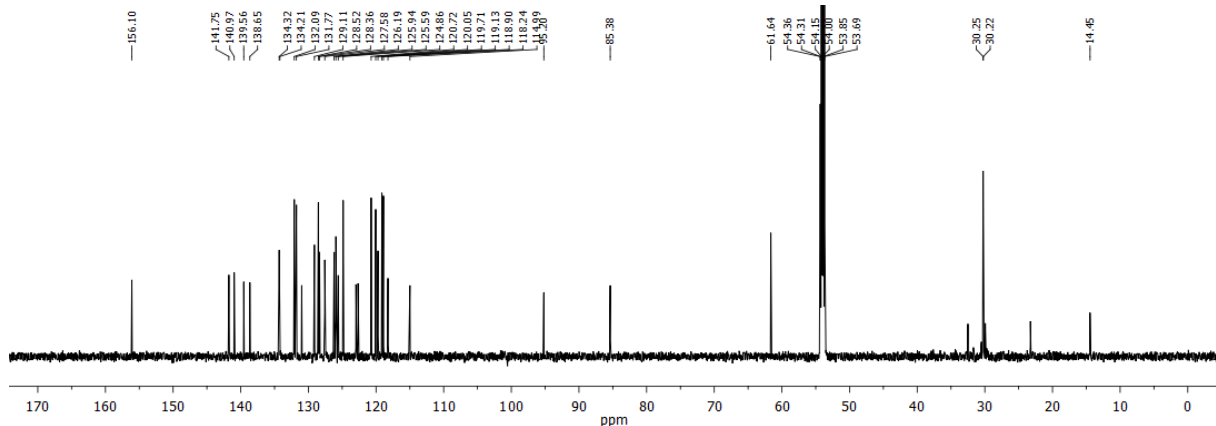


**Figure S5.**  $^{13}\text{C}\{\text{H}\}$  NMR (176 MHz,  $\text{CD}_2\text{Cl}_2$ ) of (*R*)-1.

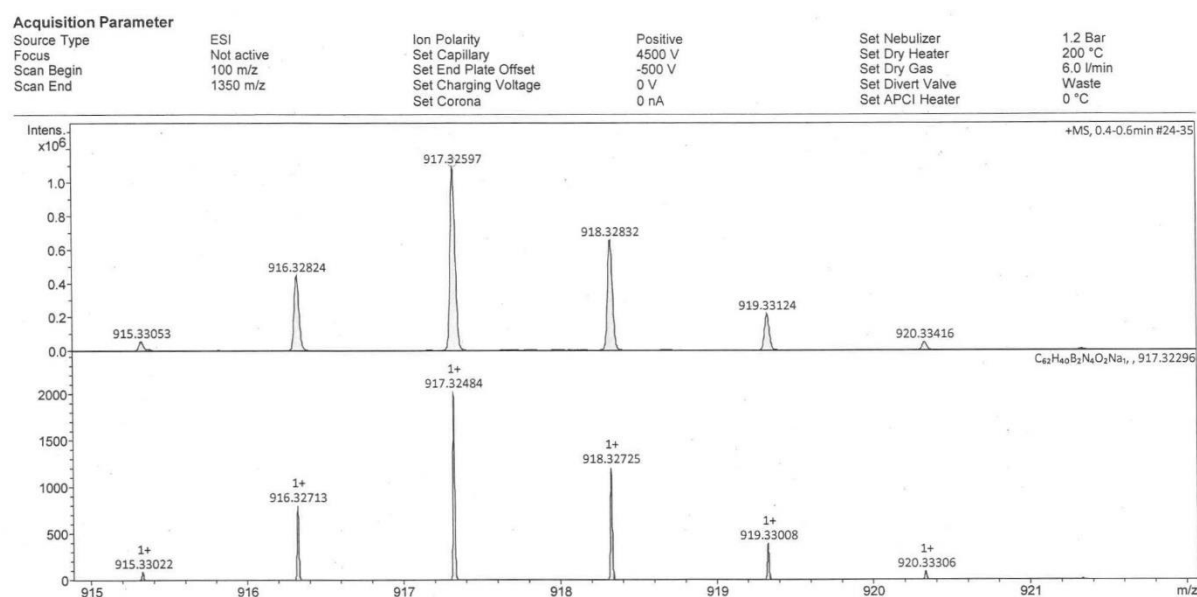


**Figure S6.** Experimental HR ESI-MS of (*R*)-1 (top) and theoretical isotopic envelopes for  $\text{C}_{62}\text{H}_{40}\text{B}_2\text{N}_4\text{O}_2\text{Na}^+$  ( $[\text{M}+\text{Na}]^+$ ) (bottom).  $m/z$   $[\text{M}+\text{Na}]^+$  calculated for  $\text{C}_{62}\text{H}_{40}\text{B}_2\text{N}_4\text{O}_2\text{Na}$ : 917.32484; found: 917.32597 ( $\Delta$ : 1.23 ppm).

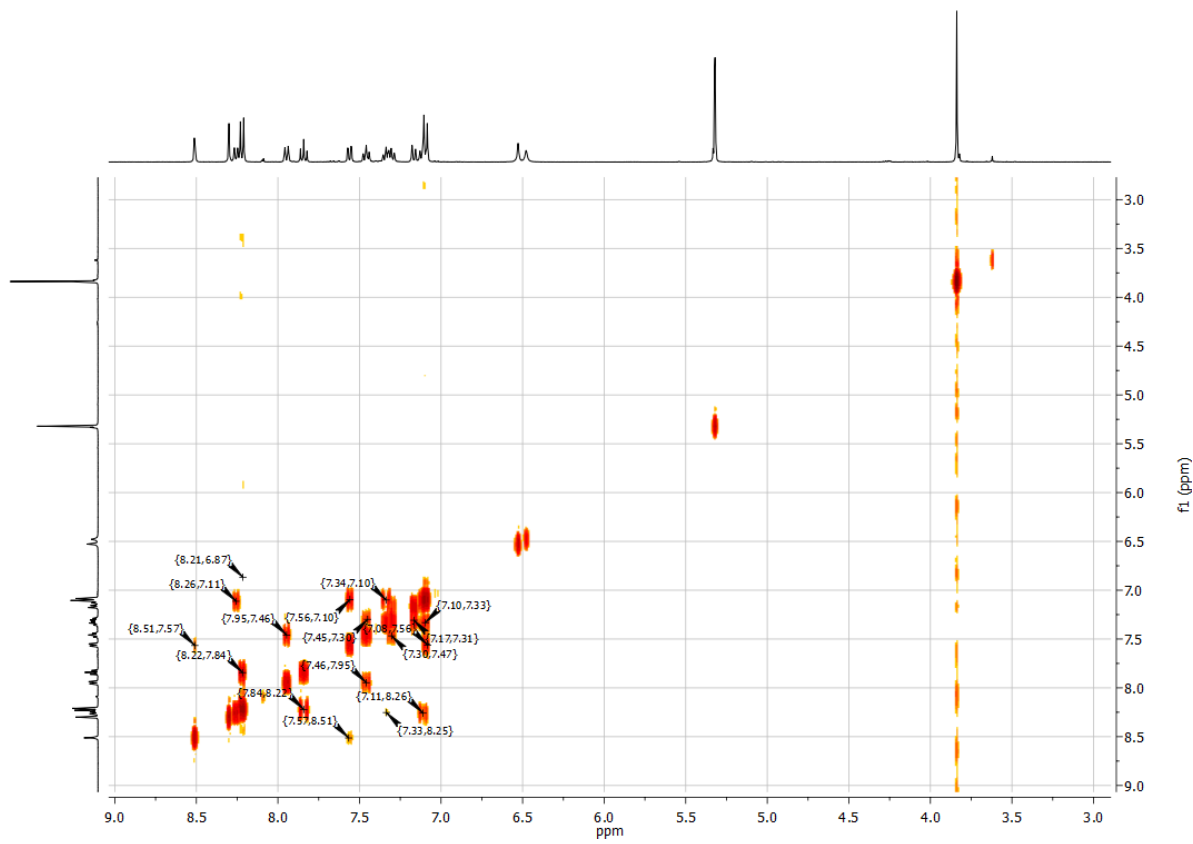


**Figure S7.** H–H-COSY NMR (400 MHz, CD<sub>2</sub>Cl<sub>2</sub>) of (*R*)-1.

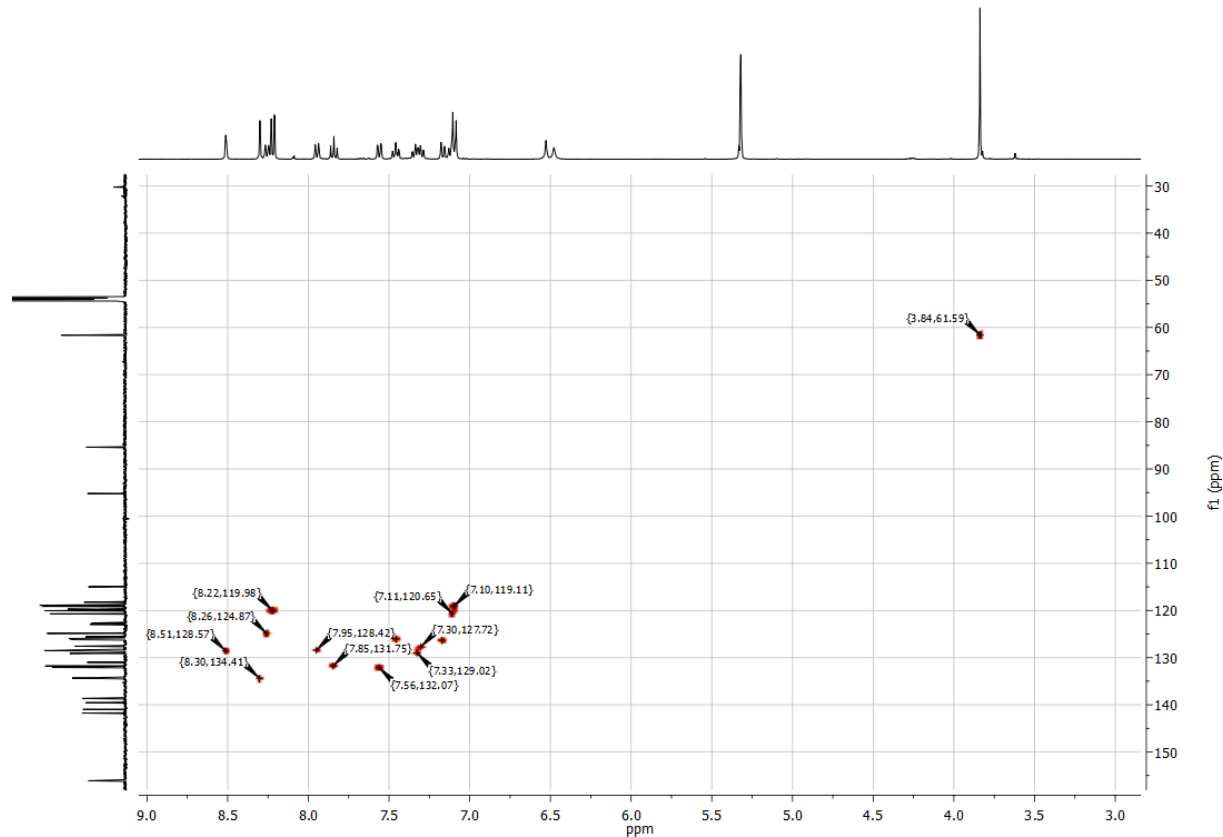


**Figure S8.** HSQC NMR (400 {101} MHz, CD<sub>2</sub>Cl<sub>2</sub>) of (*R*)-1.

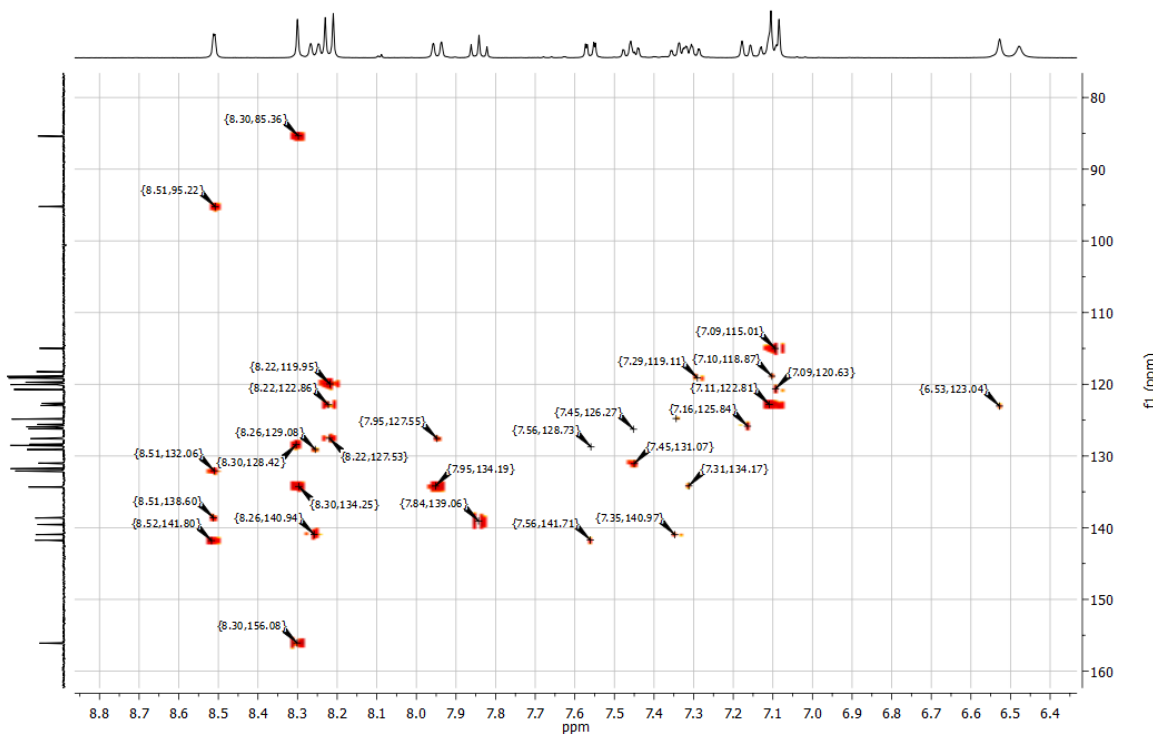


**Figure S9.** HMBC NMR (400 {101} MHz, CD<sub>2</sub>Cl<sub>2</sub>) of (*R*)-1.

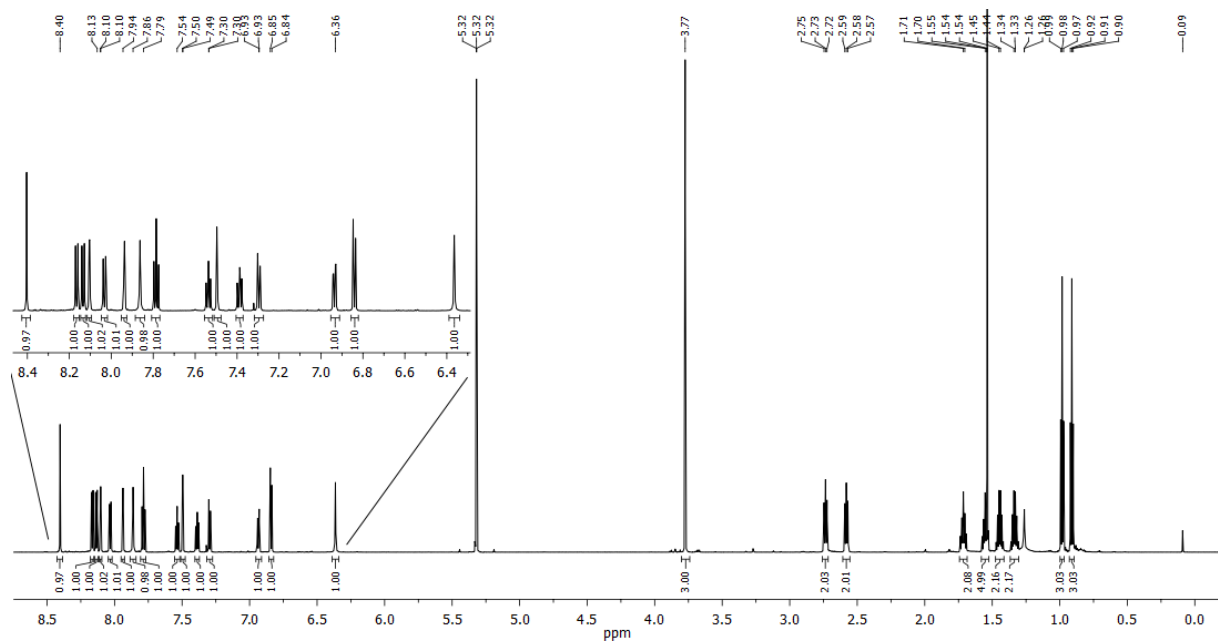


**Figure S10.**  $^1\text{H}$  NMR (700 MHz,  $\text{CD}_2\text{Cl}_2$ ) of (*S*)-2.

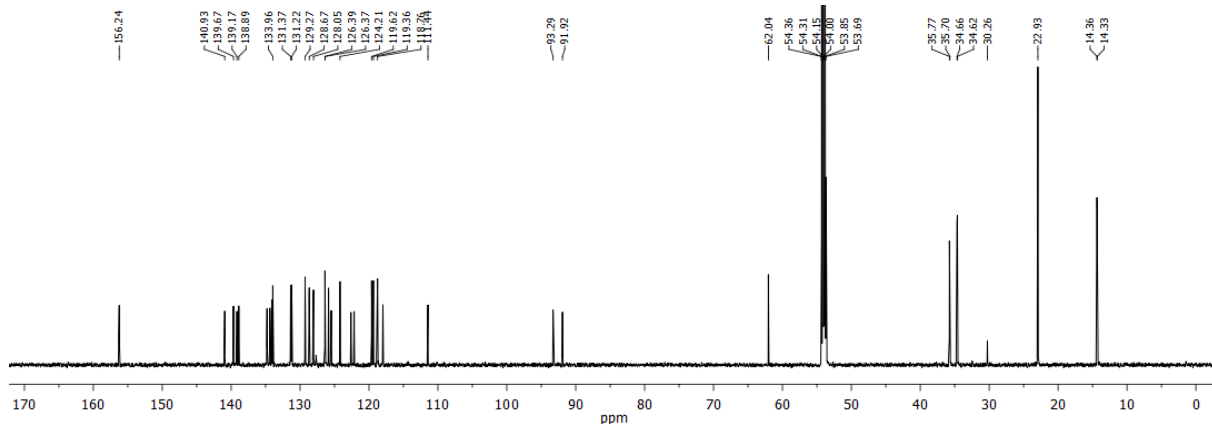


**Figure S11.**  $^{13}\text{C}\{\text{H}\}$  NMR (176 MHz,  $\text{CD}_2\text{Cl}_2$ ) of (S)-2.

Acquisition Parameter

Source Type	ESI	Ion Polarity	Positive	Set Nebulizer	0.3 Bar
Focus	Active	Set Capillary	3800 V	Set Dry Heater	200 °C
Scan Begin	260 m/z	Set End Plate Offset	-500 V	Set Dry Gas	4.0 l/min
Scan End	1500 m/z	Set Charging Voltage	0 V	Set Divert Valve	Waste
		Set Corona	0 nA	Set APCI Heater	0 °C

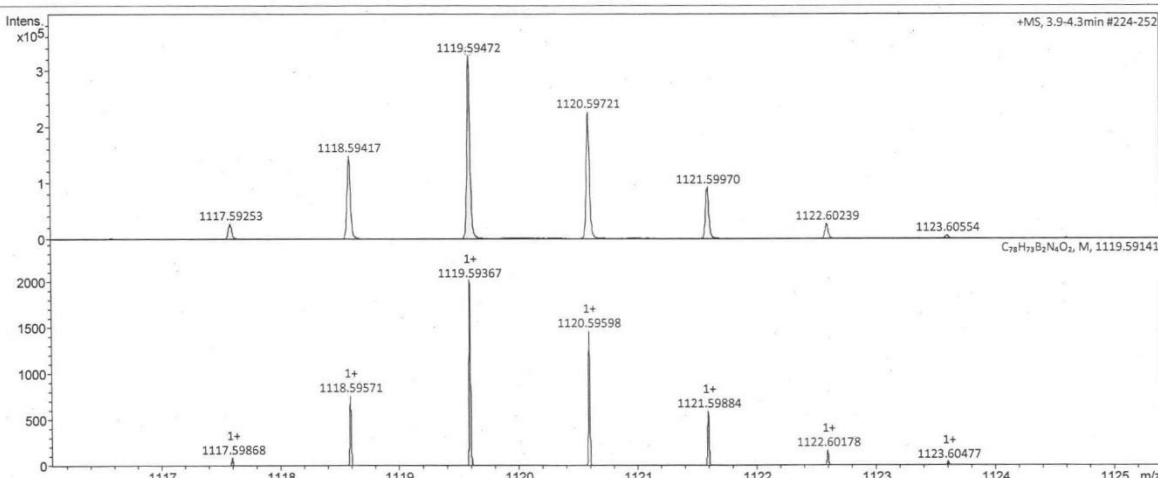


**Figure S12.** Experimental HR ESI-MS of (S)-2 (top) and theoretical isotopic envelopes for  $\text{C}_{78}\text{H}_{73}\text{B}_2\text{N}_4\text{O}_2$   $[\text{M}+\text{H}]^+$  (bottom).  $m/z$   $[\text{M}+\text{H}]^+$  calculated for  $\text{C}_{78}\text{H}_{73}\text{B}_2\text{N}_4\text{O}_2$ : 1119.59367; found: 1119.59472 ( $\Delta$ : 0.94 ppm).

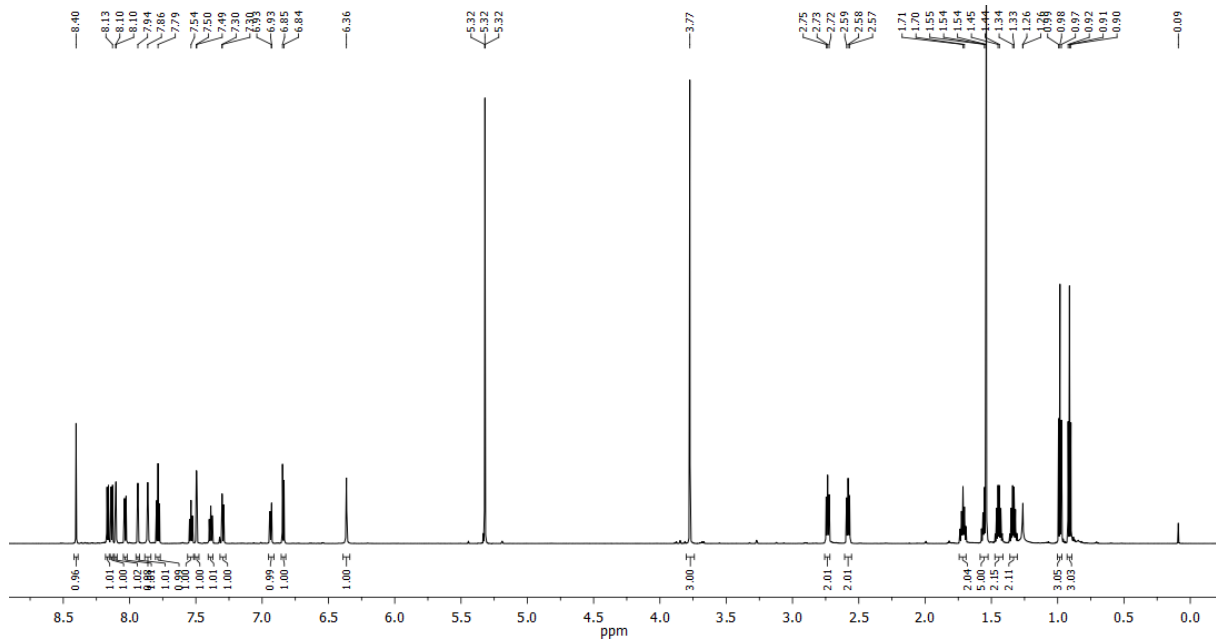


**Figure S13.**  $^1\text{H}$  NMR (700 MHz,  $\text{CD}_2\text{Cl}_2$ ) of (*R*)-2.

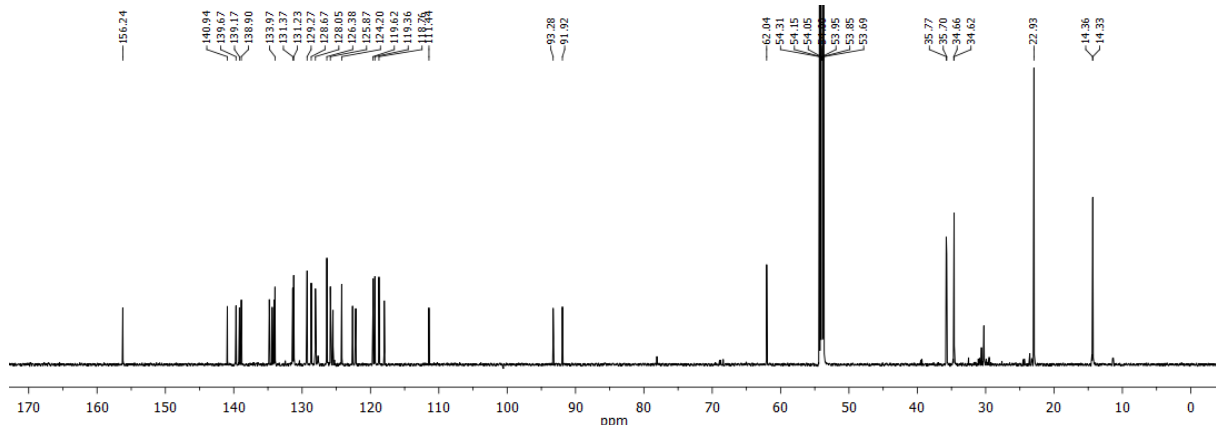


**Figure S14.**  $^{13}\text{C}\{^1\text{H}\}$  NMR (176 MHz,  $\text{CD}_2\text{Cl}_2$ ) of **(R)-2**.

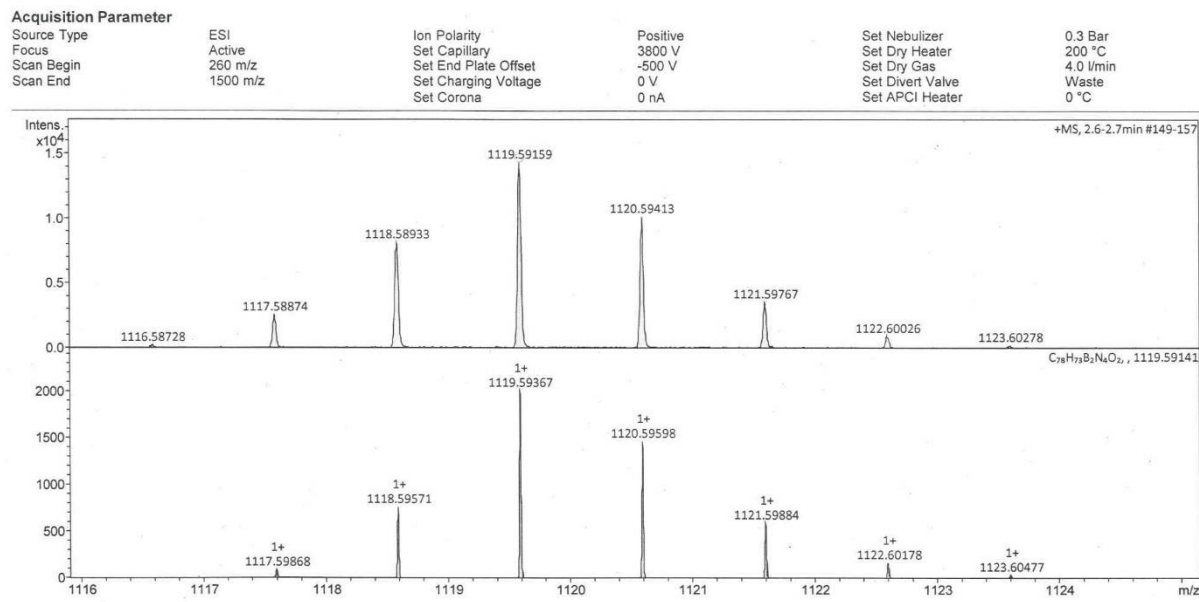


**Figure S15.** Experimental HR ESI-MS of (*R*)-2 and theoretical isotopic envelopes for  $\text{C}_{78}\text{H}_{73}\text{B}_2\text{N}_4\text{O}_2$   $[\text{M}+\text{H}]^+$  (bottom).  $m/z$   $[\text{M}+\text{H}]^+$  calculated for  $\text{C}_{78}\text{H}_{73}\text{B}_2\text{N}_4\text{O}_2$ : 1119.59367; found: 1119.59159 ( $\Delta$ : 1.86 ppm).

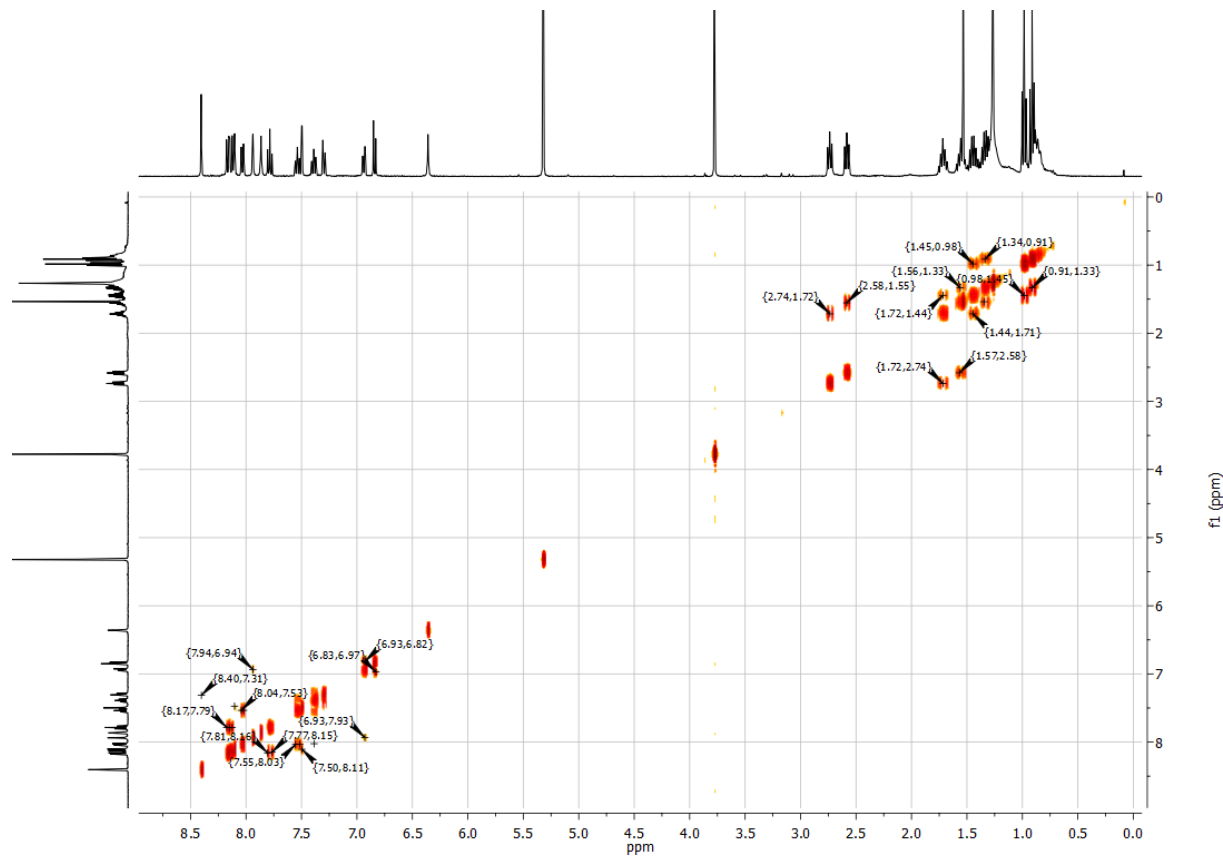


**Figure S16.** H–H-COSY NMR (400 MHz,  $\text{CD}_2\text{Cl}_2$ ) of (*R*)-2.

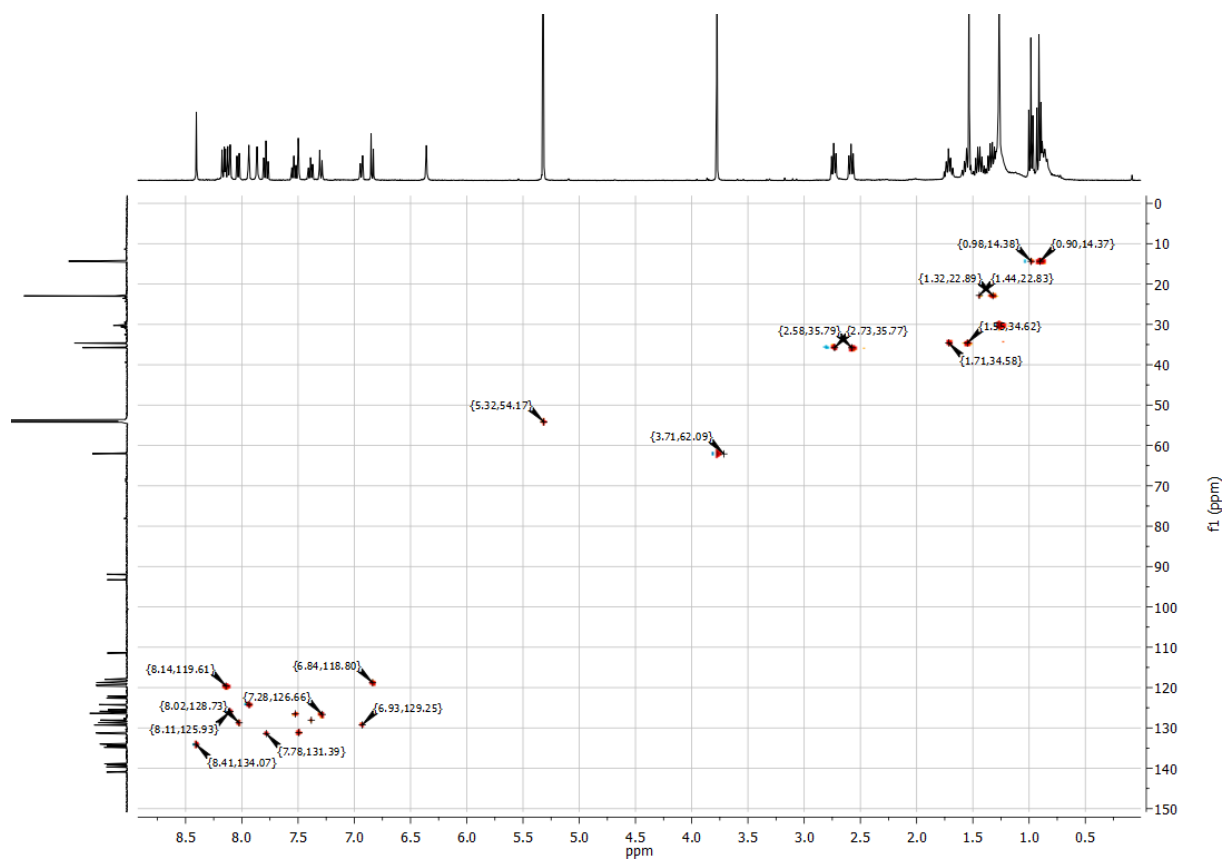


**Figure S17.** HSQC NMR (400 {101} MHz, CD<sub>2</sub>Cl<sub>2</sub>) of (**R**)-2.

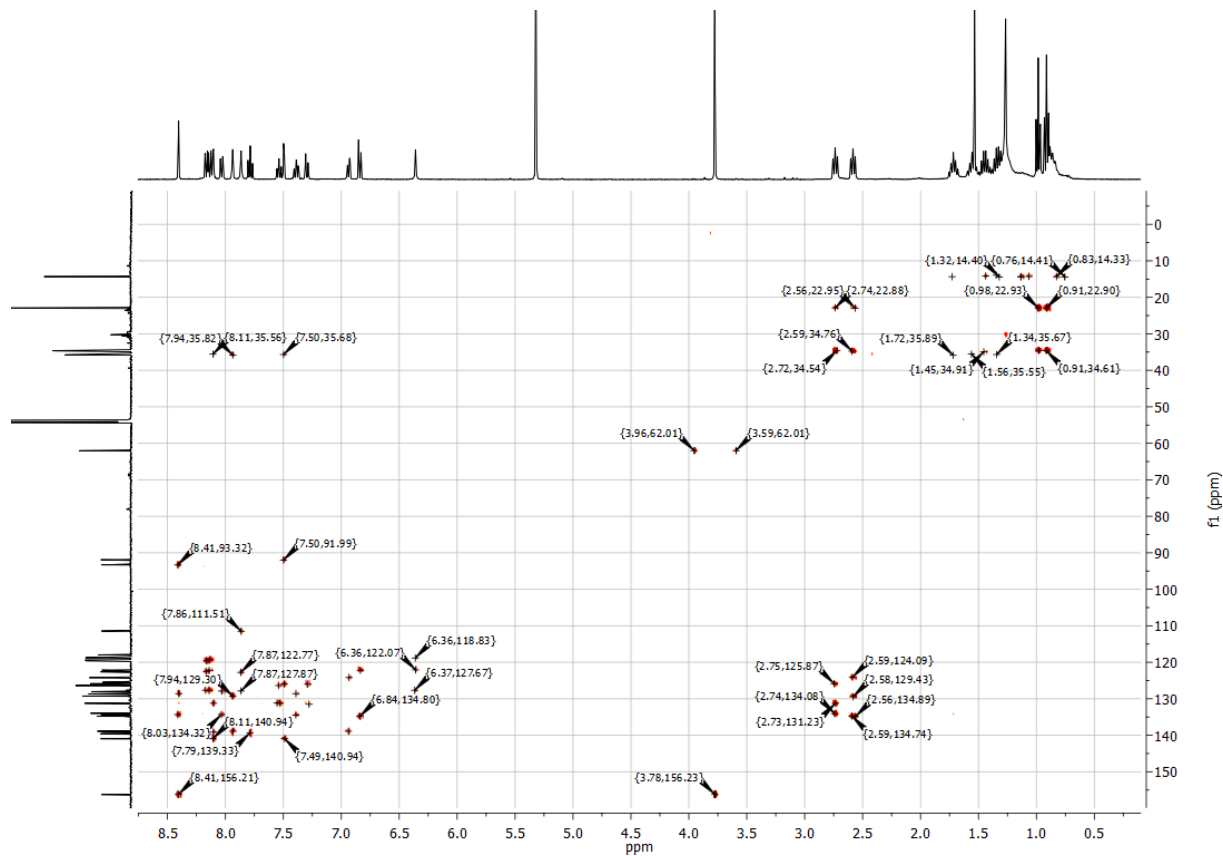


**Figure S18.** HMBC NMR (400 {101} MHz, CD<sub>2</sub>Cl<sub>2</sub>) of (**R**)-2.

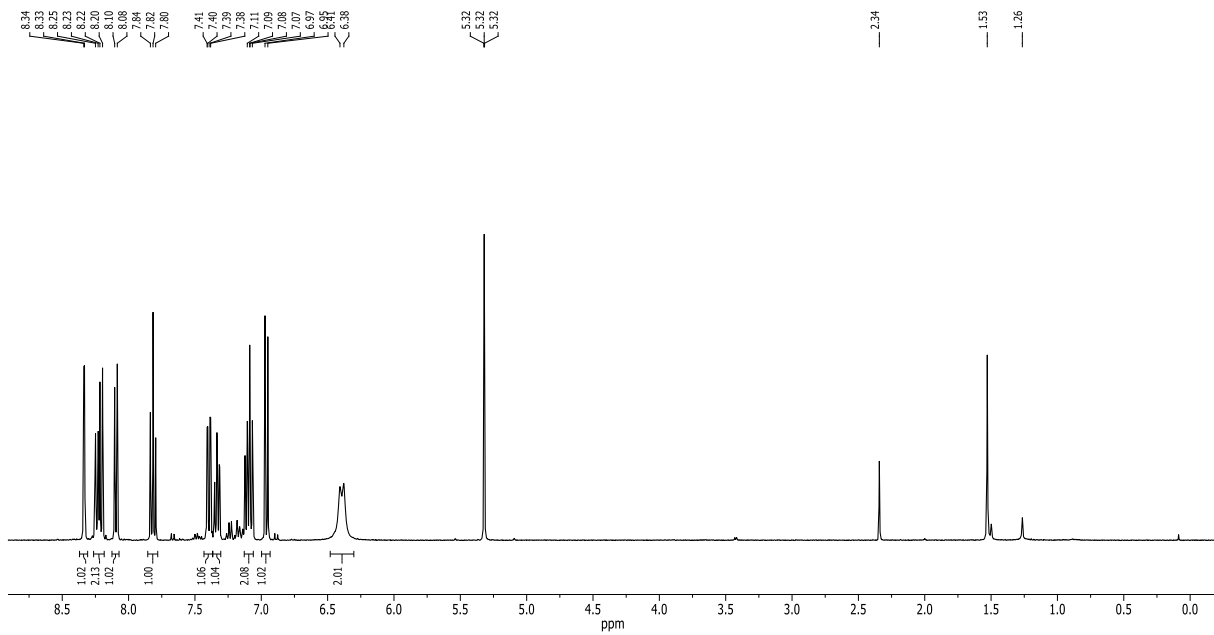


**Figure S19.**  $^1\text{H}$  NMR (400 MHz,  $\text{CD}_2\text{Cl}_2$ ) of **4**.

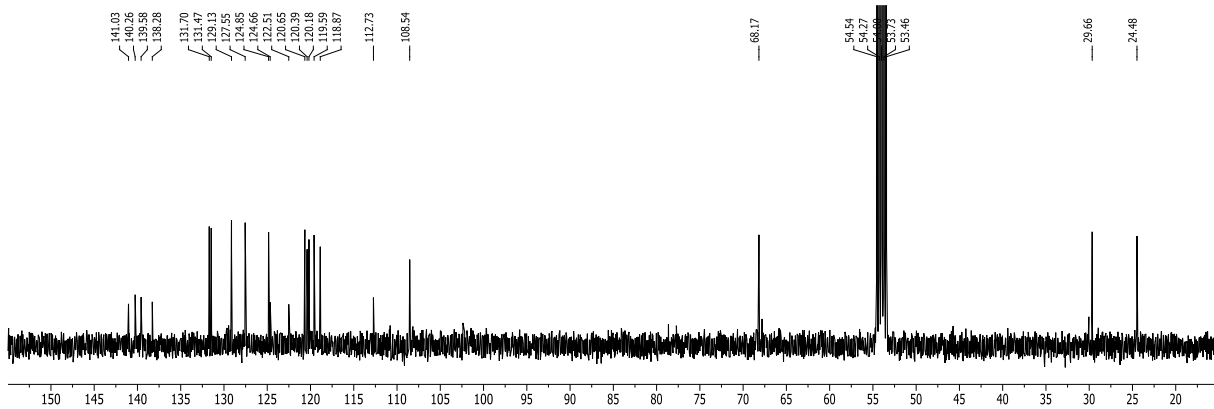


**Figure S20.**  $^{13}\text{C}\{^1\text{H}\}$  NMR (101 MHz,  $\text{CD}_2\text{Cl}_2$ ) of **4**.

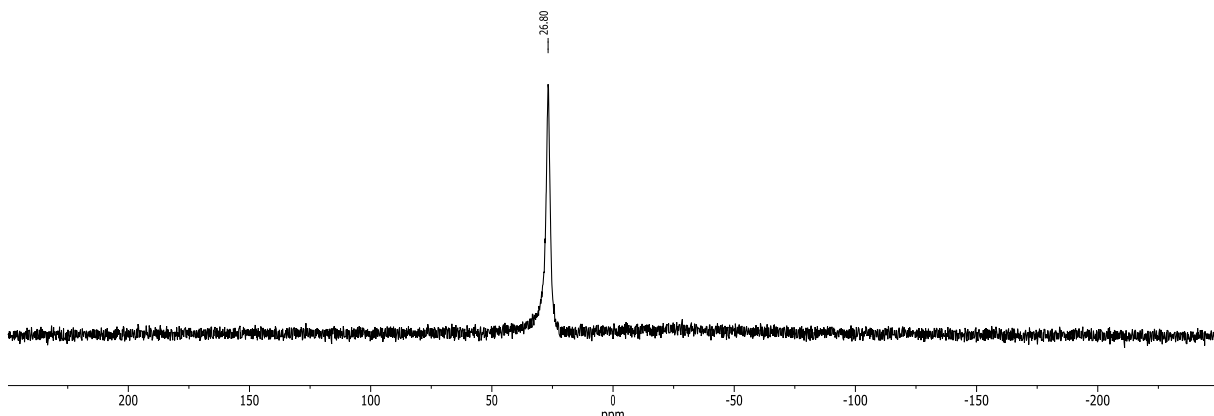


**Figure S21.**  $^{11}\text{B}\{^1\text{H}\}$  NMR (128 MHz,  $\text{CD}_2\text{Cl}_2$ ) of **4**.

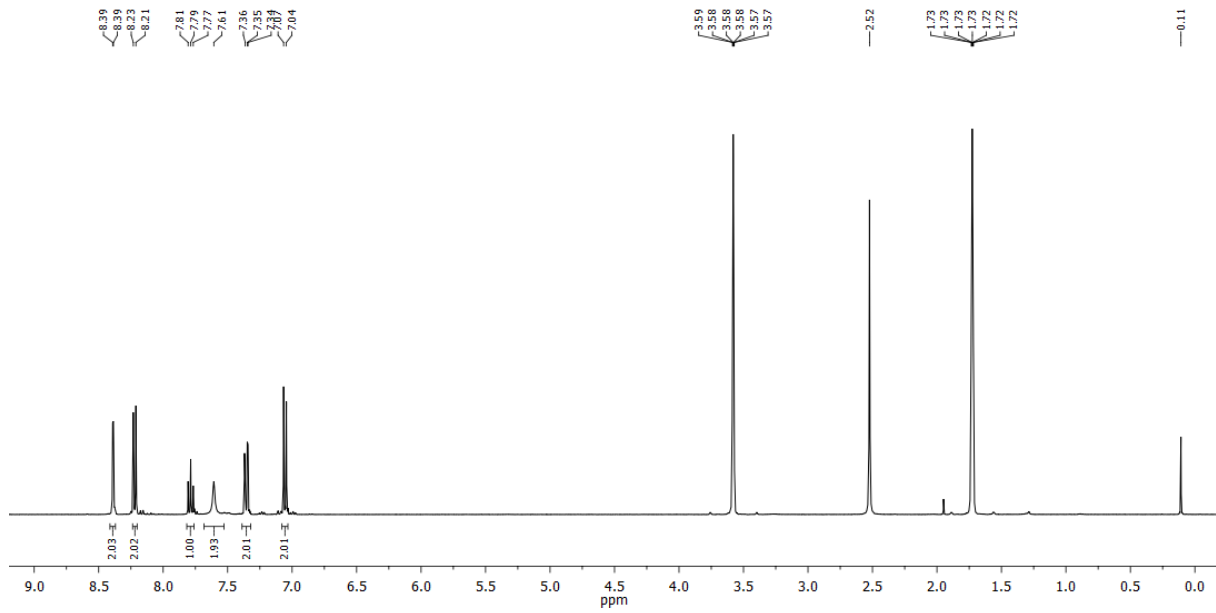


**Figure S22.**  $^1\text{H}$  NMR (400 MHz, THF- $d_8$ ) of 3,9-dibromo-NBN-benzo[*f,g*]tetracene.

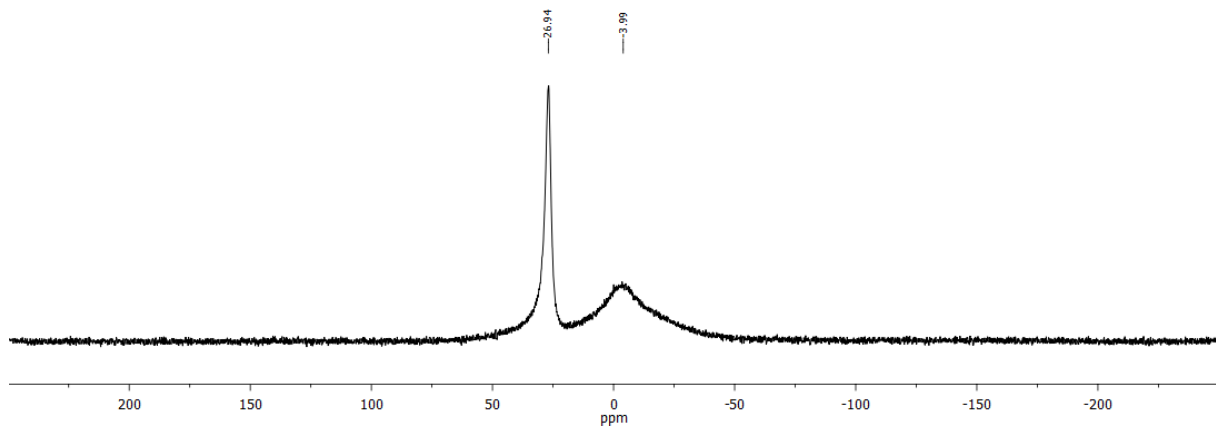


**Figure S23.**  $^{11}\text{B}\{^1\text{H}\}$  NMR (128 MHz, THF- $d_8$ ) of 3,9-dibromo-NBN-benzo[*f,g*]tetracene. The broad signal at -3.99 ppm is related to the boron-silica NMR glass tube.

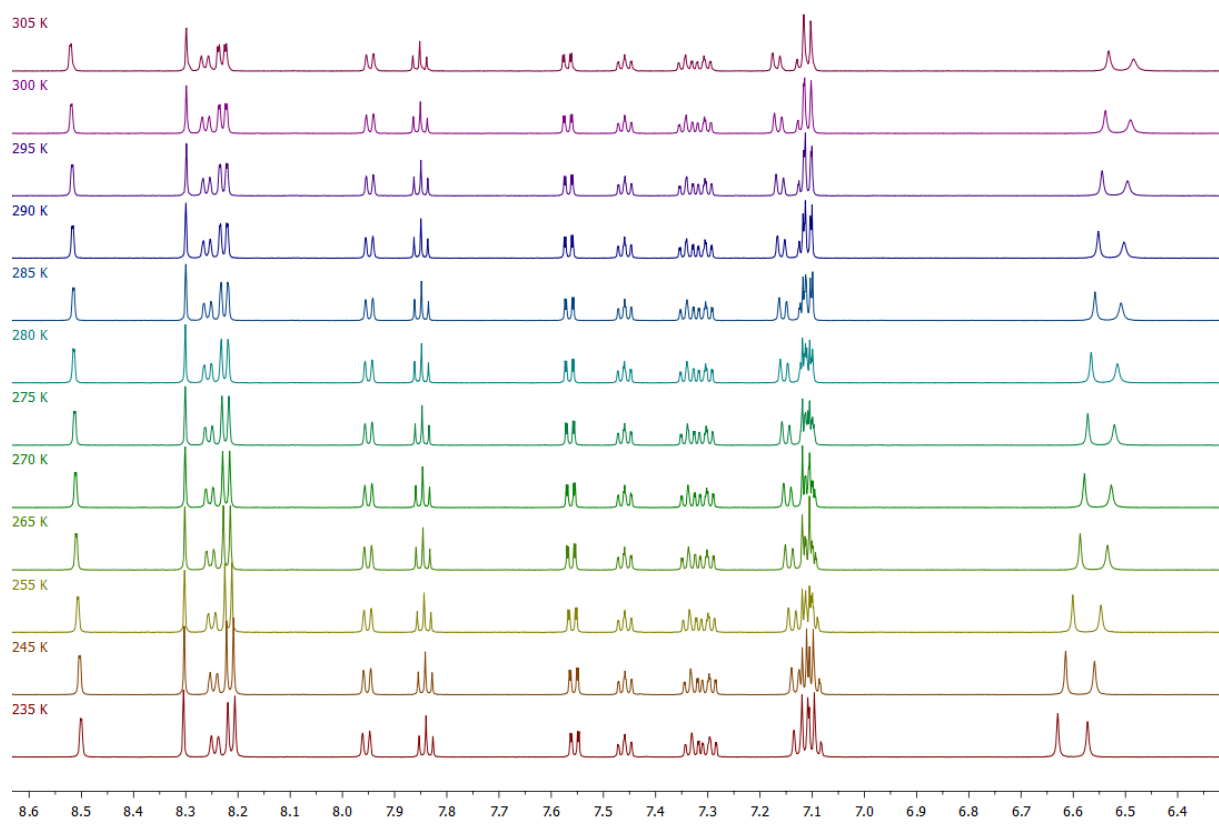


**Figure S24.** Variable-temperature <sup>1</sup>H NMR (600 MHz, CD<sub>2</sub>Cl<sub>2</sub>) of (*R*)-1 from 235–305 K.

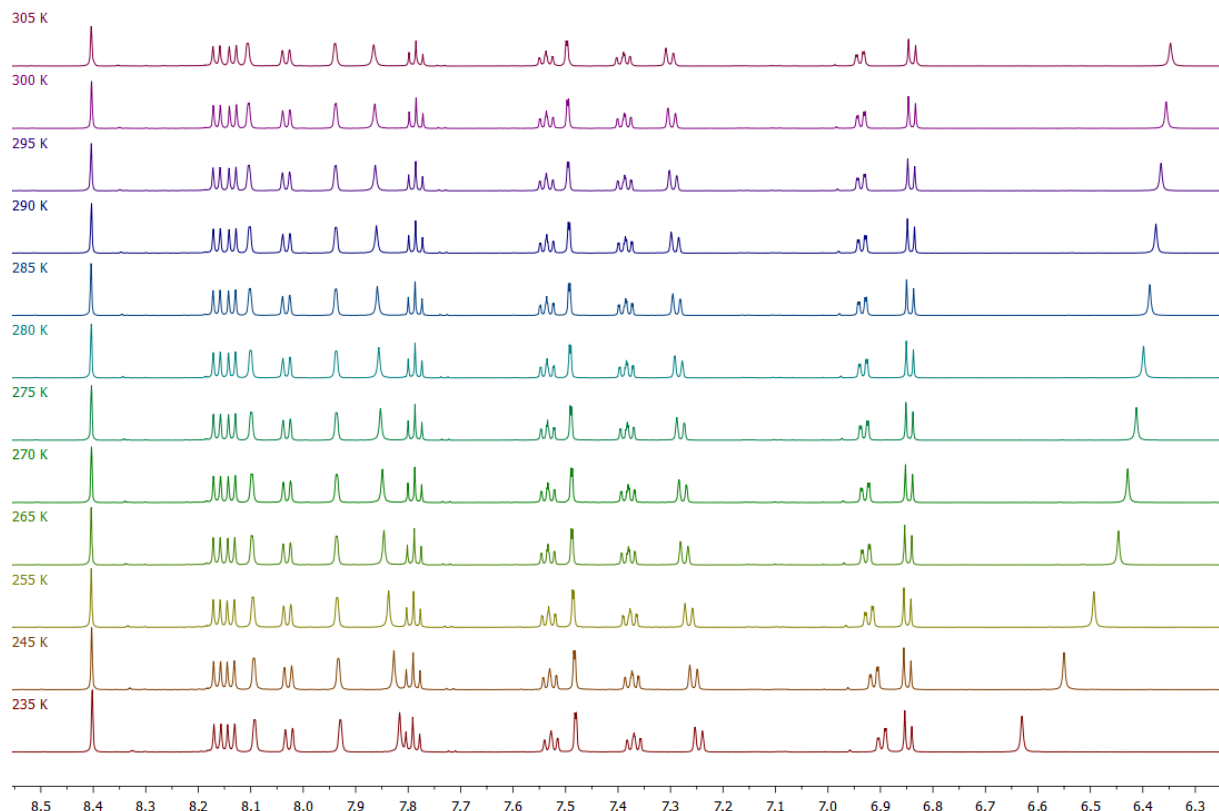


**Figure S25.** Variable-temperature <sup>1</sup>H NMR (600 MHz, CD<sub>2</sub>Cl<sub>2</sub>) of (*R*)-2 from 235–305 K.

### 3. Optical Spectra: Photoluminescence lifetimes, $g_{lum}$ -vs-wavelength

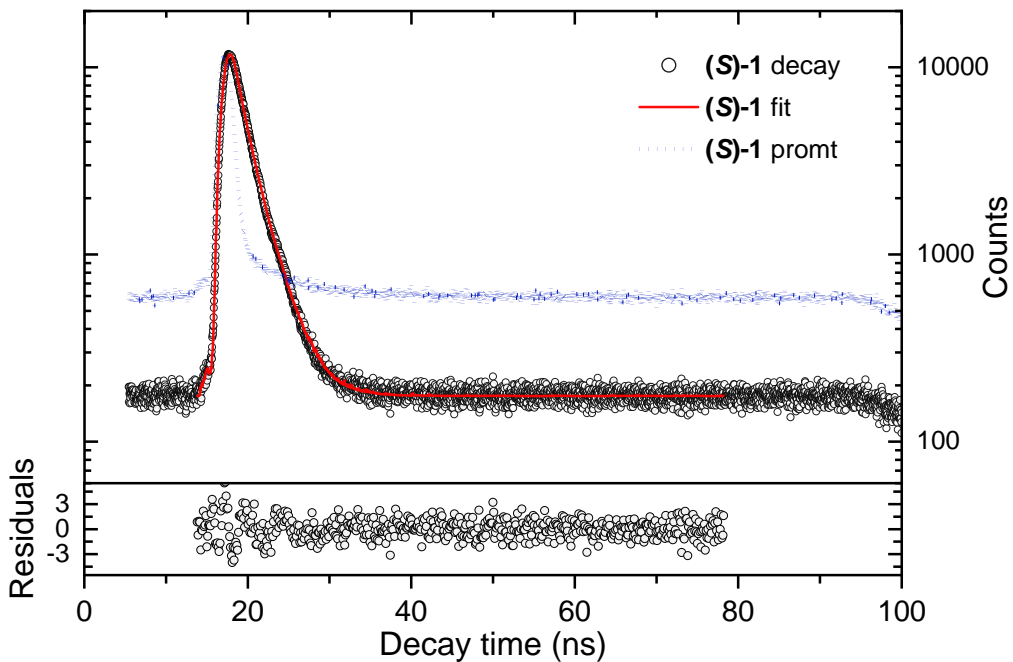


**Figure S26.** Time-resolved photoluminescence decay curves of (S)-1. The decay is best fitted to a biexponential equation ( $\chi^2 = 1.52$ ) with 0.07 ns,\* 1.82 ns (30 % and 70 % relative amplitudes, respectively), considering the instruments response function (IRF) by an iterative deconvolution fitting method. \*data artifact

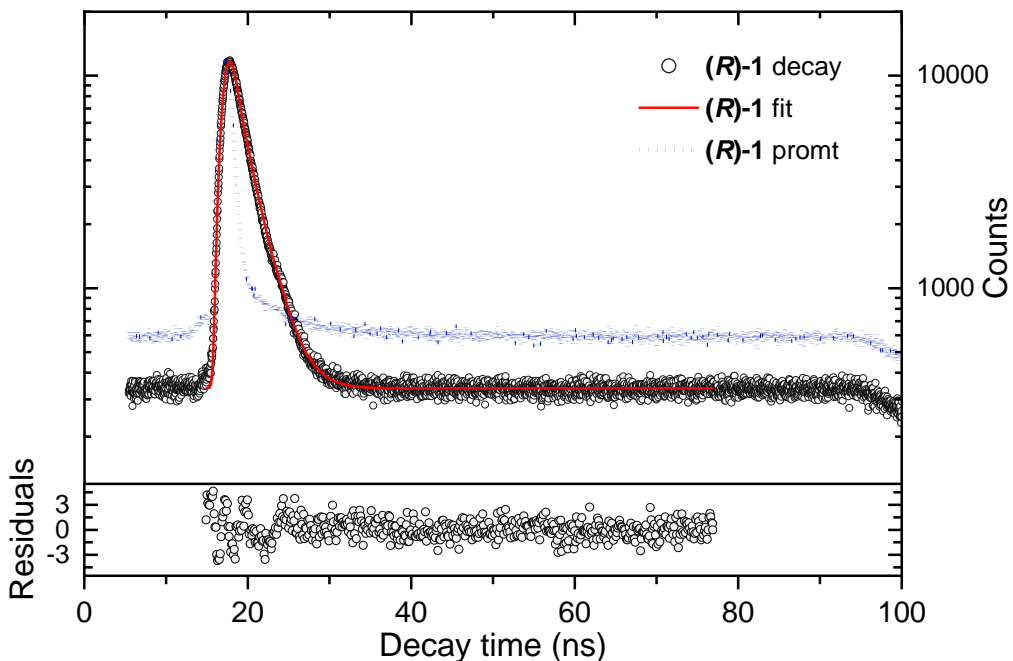


**Figure S27.** Time-resolved photoluminescence decay curves of (R)-1. The decay is best fitted to a biexponential equation ( $\chi^2 = 1.65$ ) with 0.14 ns,\* 1.91 ns (28 % and 72 % relative amplitudes, respectively), considering the instruments response function (IRF) by an iterative deconvolution fitting method. \*data artifact

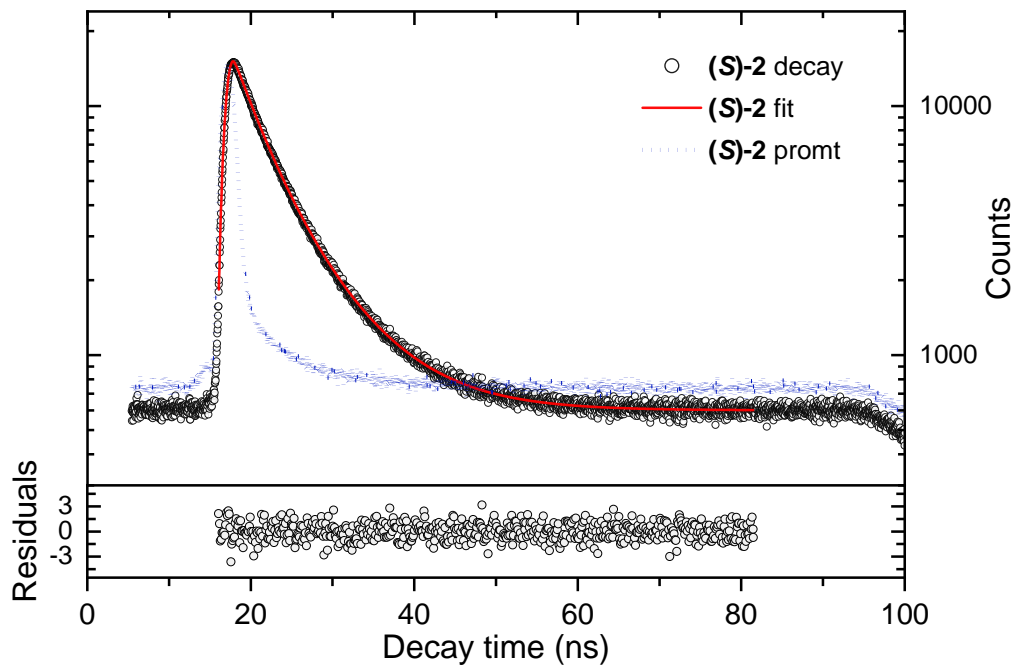


**Figure S28.** Time-resolved photoluminescence decay curves of **(S)-2**. The decay is best fitted to triexponential equation ( $\chi^2 = 1.12$ ) with  $\tau = 0.33$  ns,\* 3.43 ns, and 7.52 ns (-2 %, 40 % and 62 % relative amplitudes, respectively), considering the instruments response function (IRF) by an iterative deconvolution fitting method. \*data artifact

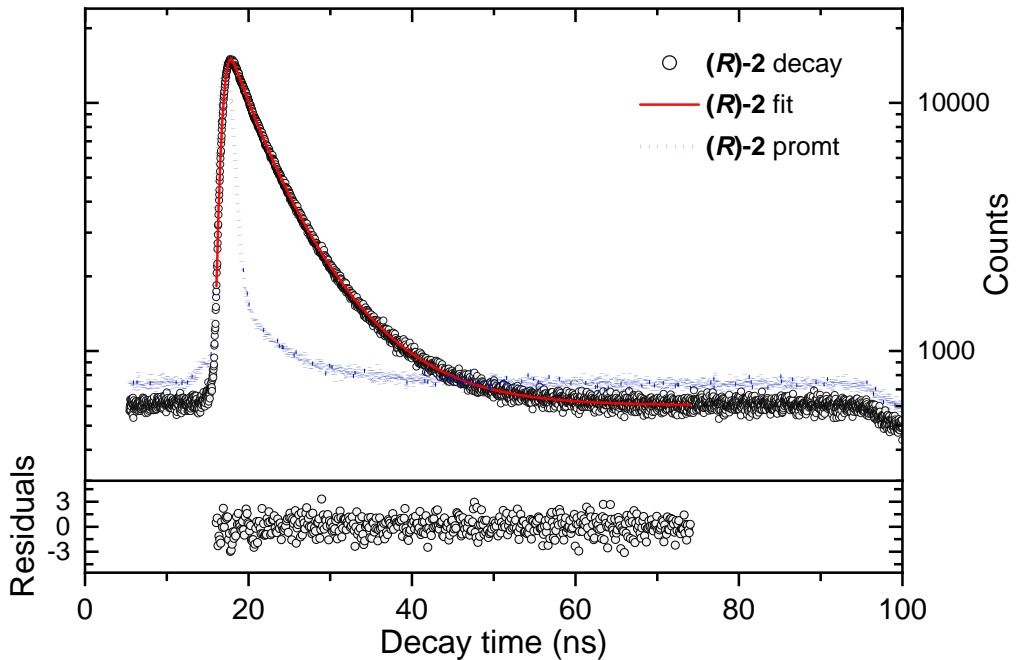


**Figure S29.** Time-resolved photoluminescence decay curves of **(R)-2**. The decay is best fitted to triexponential equation ( $\chi^2 = 1.02$ ) with  $\tau = 0.38$  ns,\* 3.25 ns, and 7.41 ns (-2 %, 38 %, and 64 % relative amplitudes, respectively), considering the instruments response function (IRF) by an iterative deconvolution fitting method. \*data artifact

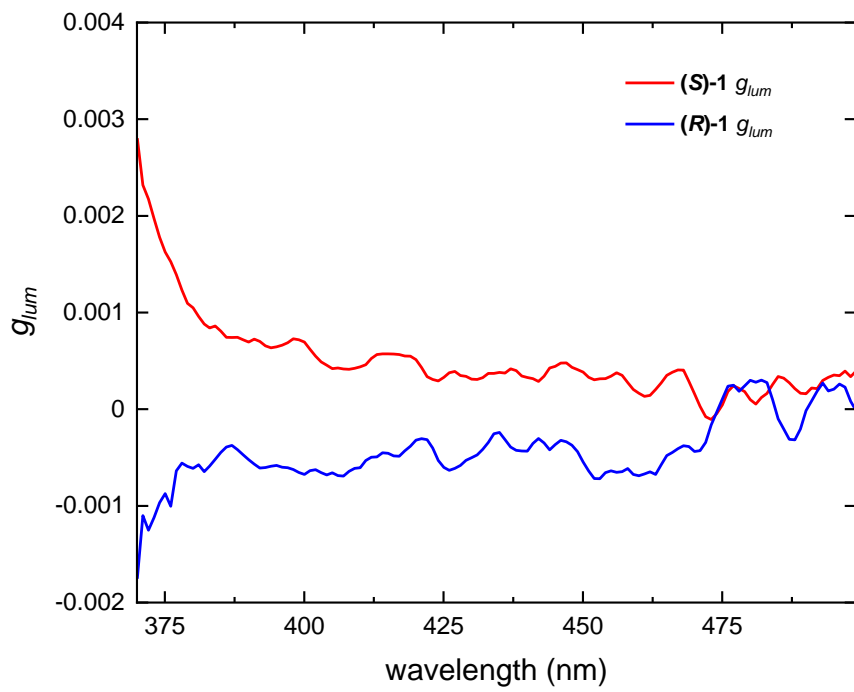


**Figure S30.**  $g_{lum}$ -vs-wavelength plot of **1**.

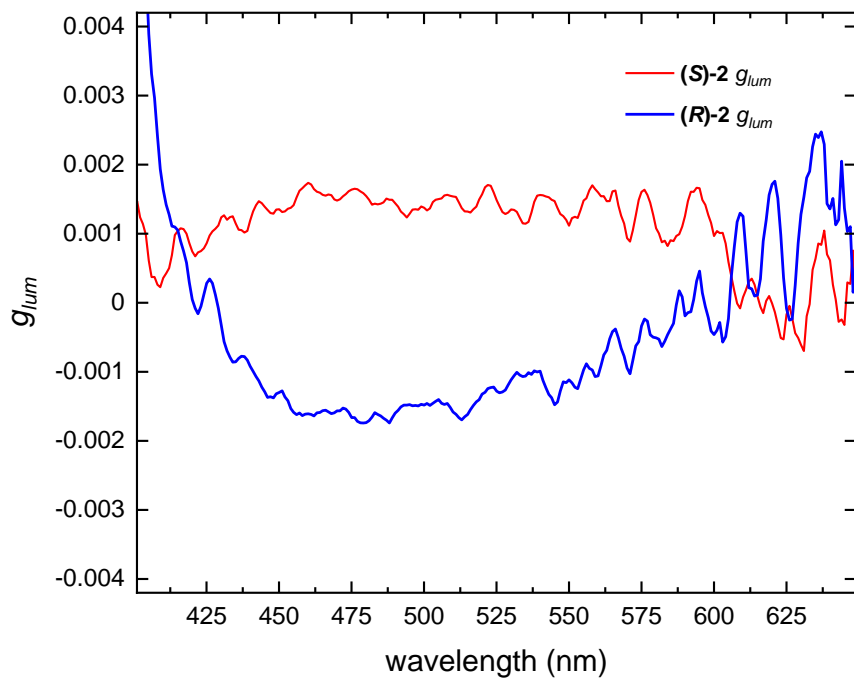


**Figure S31.**  $g_{lum}$ -vs-wavelength plot of **2**.

#### 4. Computational studies

##### Frontier Molecular Orbitals and Natural Transition Orbitals

The frontier molecular orbitals of **1** and **2'** (*n*-Bu groups replaced with H) were computed in subsequent single point computations using the M06-2X<sup>7</sup> hybrid density functional in conjunction with the def2-SV(P) basis set with the ORCA 5 program (Figure S32, Figure S33).<sup>8–10</sup> The prior geometry optimizations were performed at the same level of theory.

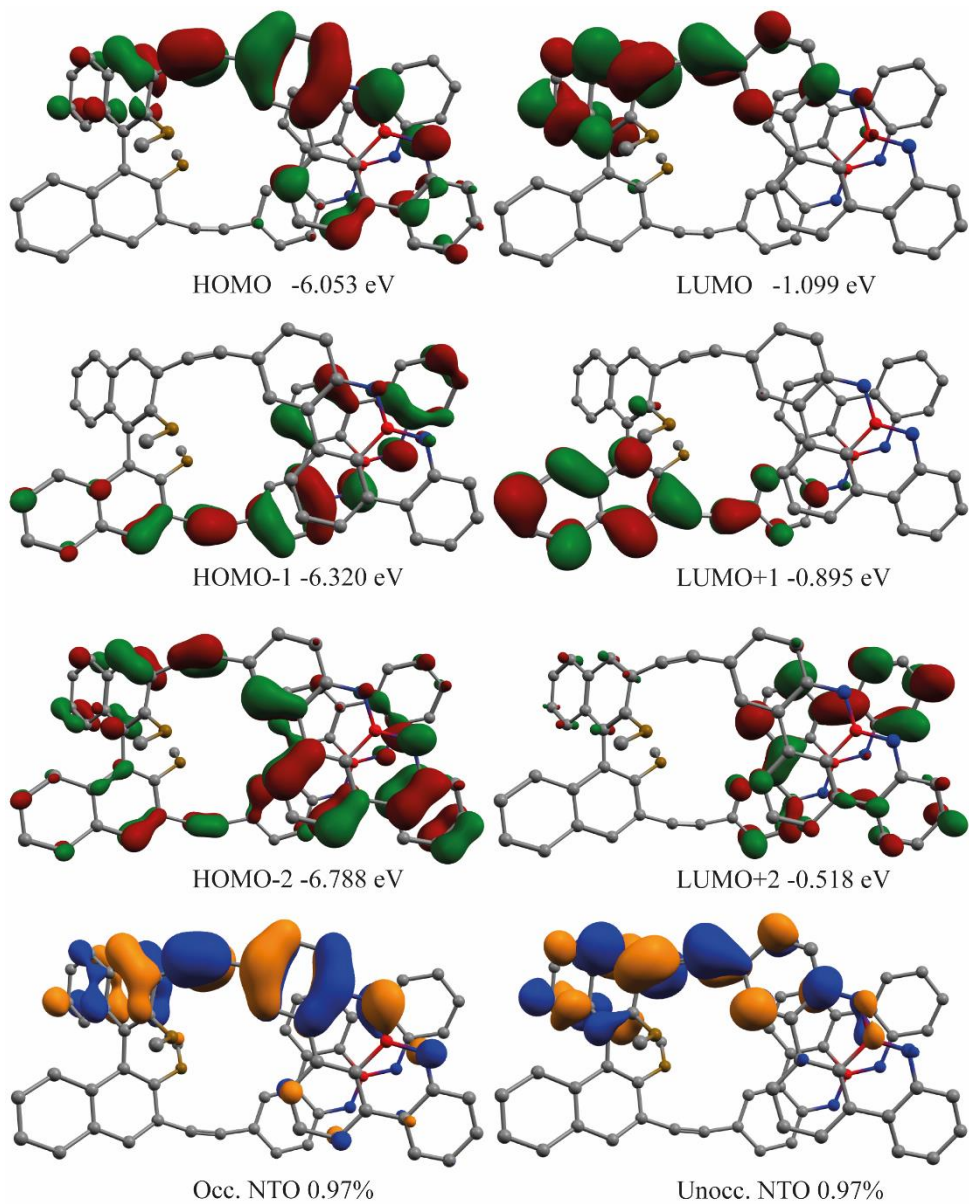


**Figure S32.** Frontier molecular orbitals and their energies and NTOs with relative contributions to the lowest energy transition of **(R)-1** as computed at the M06-2X/def2-SV(P) level of theory. For clarity, hydrogen atoms are omitted. Contour values plotted at 0.03.

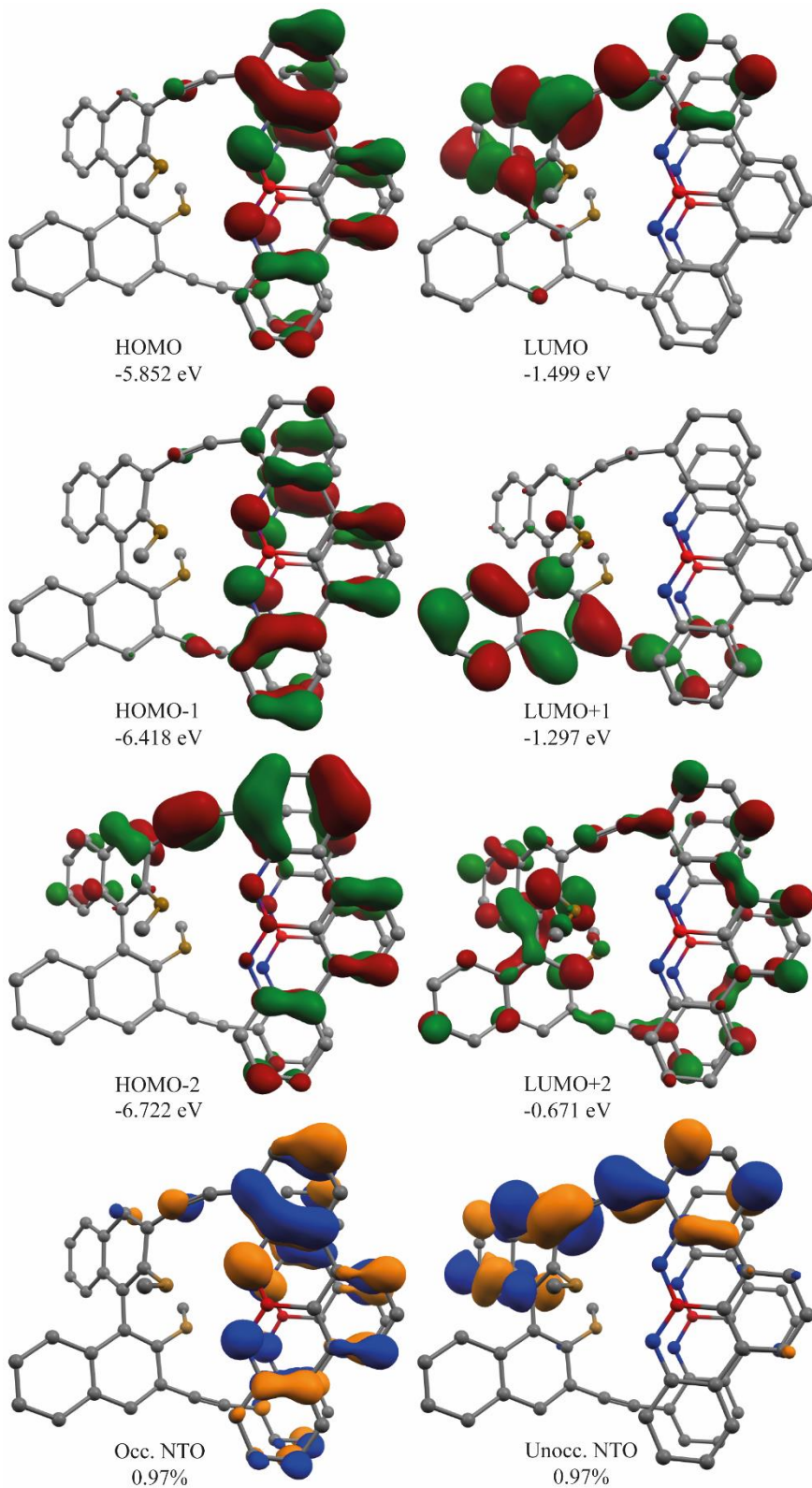


**Figure S33.** Frontier molecular orbitals and their energies and NTOs with relative contributions to the lowest energy transition of **(R)-2'** as computed at the M06-2X/def2-SV(P) level of theory. *n*-Bu groups are replaced with H. For clarity, hydrogen atoms are omitted. Contour values plotted at 0.03.

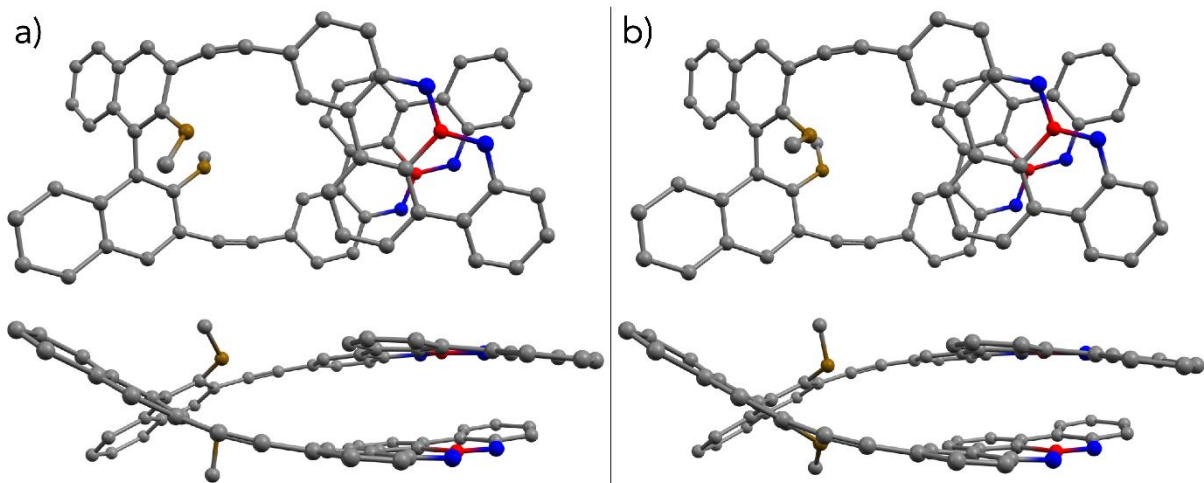


**Figure S34.** a) Ground state and b) first excited state structures of **1** under state-specific equilibrium solvation in  $\text{CH}_2\text{Cl}_2$  as computed at the M06-2X/def2-SV(P) level of theory. For clarity, hydrogen atoms are omitted.

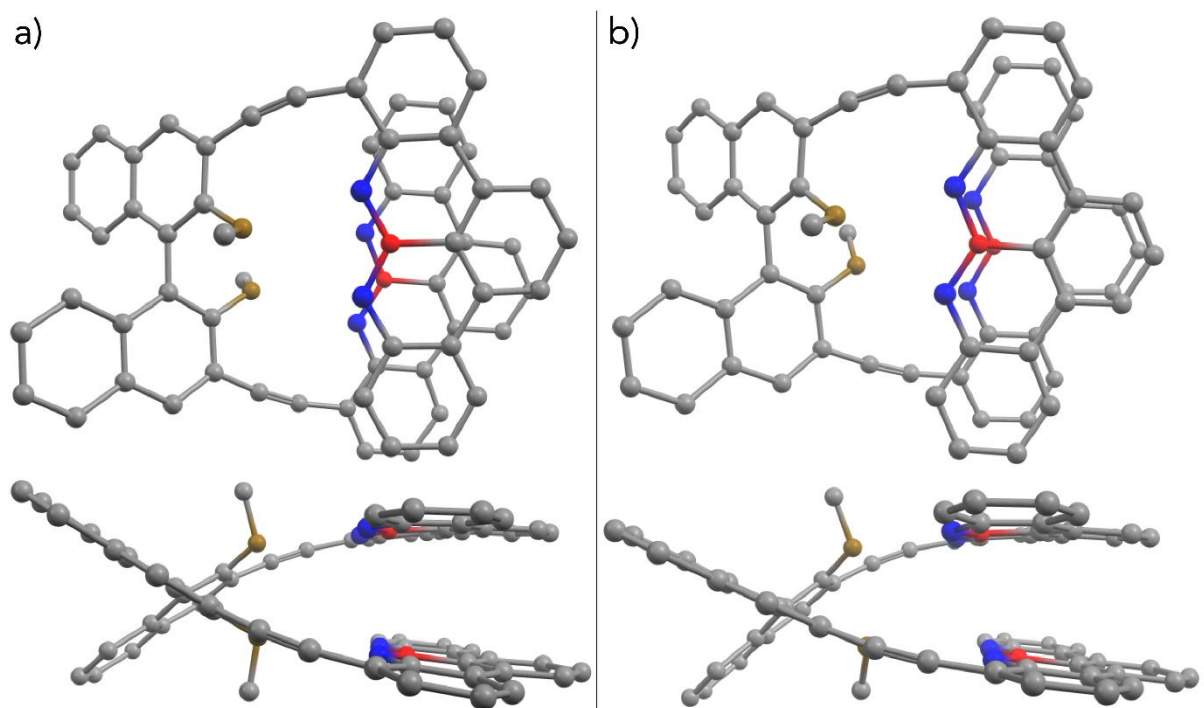


**Figure S35.** a) Ground state and b) first excited state structures of **2'** under state-specific equilibrium solvation in  $\text{CH}_2\text{Cl}_2$  as computed at the M06-2X/def2-SV(P) level of theory. For clarity, hydrogen atoms are omitted.

## Conformer Analysis with CREST and CENSO

The structures were preoptimized utilizing the semiempirical tight binding GFN-xTB method.<sup>11,12</sup> The obtained geometries were subjected to the conformer-rotamer ensemble sample tool (CREST)<sup>13,14</sup> at the GFN-xTB level of theory with CH<sub>2</sub>Cl<sub>2</sub> as solvent using the XTB<sup>11</sup> program. The conformer ensemble thus obtained was subsequently refined and sorted using the command line energetic sorting (CENSO) program<sup>15</sup> to compute the Boltzmann distribution of populated conformers. The computations were performed with the ORCA 5 software<sup>8–10</sup> and the continuum solvation model (SMD)<sup>16</sup> was applied to simulate solvation in CH<sub>2</sub>Cl<sub>2</sub>.

For the CREST computations standard parameters were applied. The obtained CREST conformers were fed into the CENSO program and part 0, part 1, and part 2 were performed with the following settings:

---

---

### CENSO PARAMETERS

---

---

### CRE SORTING SETTINGS

---

solvent:	ch2cl2
temperature:	298.15
evaluate at different temperatures:	on
temperature range:	273.15, 278.15, 283.15, 288.15, ...
calculate mRRHO contribution:	on
consider symmetry for mRRHO contribution:	on
cautious checking for error and failed calculations:	on
checking the DFT-ensemble using CREST:	off
maxthreads:	4
omp:	12
automatically balance maxthreads and omp:	on

---

## **CRE CHEAP-PRESCREENING - PART0**

---

part0:	on
program for part0:	orca
functional for fast single-point:	b97-d3
basis set for fast single-point:	def2-SV(P)
threshold g_thr(0) for sorting in part0:	4.0
Solvent model used with xTB:	alpb
short-notation:	
b97-d3/def2-SV(P) // GFNn-xTB (Input geometry)	

---

## **CRE PRESCREENING - PART1**

---

part1:	on
program for part1:	orca
functional for initial evaluation:	r2scan-3c
basis set for initial evaluation:	def2-mTZVPP
calculate mRRHO contribution:	on
program for mRRHO contribution:	xtb
GFN version for mRRHO and/or GBSA_Gsolv:	gfn2
Apply constraint to input geometry during mRRHO calculation:	on
solvent model applied with xTB:	alpb
evaluate at different temperatures:	off
threshold g_thr(1) and G_thr(1) for sorting in part1:	3.5
solvent model for Gsolv contribution of part1:	smd

short-notation:

r2scan-3c + SMD[ch2cl2] + GmRRHO(GFN2[alpb]-bhess) // GFNn-xTB (Input geometry)

---

## CRE OPTIMIZATION - PART2

---

part2:	on
program:	orca
QM program employed only in the geometry opt.:	orca
functional for part2:	r2scan-3c
basis set for part2:	def2-mTZVPP
using xTB-optimizer for optimization:	on
using the new ensemble optimizer:	on
optimize all conformers below this G_thr(opt,2) threshold:	2.5
spearmanthr:	0.907
optimization level in part2:	lax
solvent model applied in the optimization:	smd
solvent model for Gsolv contribution:	smd
evaluate at different temperatures:	on
Boltzmann sum threshold G_thr(2) for sorting in part2:	99.0
calculate mRRHO contribution:	on
program for mRRHO contribution:	xtb
GFN version for mRRHO and/or GBSA_Gsolv:	gfn2
Apply constraint to input geometry during mRRHO calculation:	on
solvent model applied with xTB:	alpb
short-notation:	

r2scan-3c + SMD[ch2cl2] + GmRRHO(GFN2[alpb]-bhess) // r2scan-3c[SMD]

According to CENSO, for **1** and **2'**, the sole populated conformer at room temperature is similar to the respective optimized lowest-energy structure at the M06-2X/def2-SV(P) level of theory, respectively (Figure S32Figure **S33**).

### Dissymmetry Factor $g_{\text{lum,calcd}}$ .

For detailed information on the procedure to calculate the  $g_{\text{lum}}$  value of compounds we refer to Kubo et al.<sup>17</sup> The geometries of the  $S_1$  states were optimized by analytic gradients<sup>18,19</sup> using TD-DFT along with the def2-SV(P)<sup>12</sup> basis set. The meta-hybrid GGA M06-2X<sup>7</sup> functional was used. The Polarizable Continuum Model (PCM) using the integral equation formalism variant (IEFPCM) was used to simulate an equilibrium solvent reaction field during optimization of the first excited state.<sup>20–23</sup> The TD-DFT calculation from this excited state to the ground state for the transition moments needed for  $g_{\text{lum,calcd}}$  was performed under state-specific equilibrium solvation of the excited state at its equilibrium geometry. Using the corrected linear-response approach, the ground state energy at the excited state geometry was computed under non-equilibrium solvation with the static solvation from the excited state. The difference between the excited state and the ground state energy, both under excited state geometry and solvation correction, gives the vertical emission energy  $E_{\text{ex}}$ . These computations were run with the Gaussian 16 package.<sup>24</sup>

The dissymmetry factor  $g_{\text{lum,calcd}}$  was calculated as follows:  $g = 4R/(D+G)$ . R is the rotatory strength defined by the inner product of transition electric and magnetic dipole moments (it can be either calculated via  $R = |\mu_e| \cdot |\mu_m| \cdot \cos\theta$  or taken from the highlighted R(length) column in Table S1 and Table S2, and D and G are the electric and magnetic dipole strengths defined by the square of transition electric and magnetic dipole moments, respectively ( $D = |\mu_e|^2$ ;  $G = |\mu_m|^2$ ).

**Table S1.** Cartesian coordinates (Å) and transition moments of the optimized structure of (**R**)-**1** in CH<sub>2</sub>Cl<sub>2</sub> in the lowest-energy excited state ( $S_1$ ) calculated at the M06-2X/def2-SV(P) level of theory.

Center Number	Atomic Number	Atomic Type	Coordinates (Angstroms)		
			X	Y	Z
1	6	0	-5.618028	-3.367379	-0.955495
2	6	0	-7.472030	-1.322083	-1.195418
3	6	0	-7.899157	-2.601443	-0.870638
4	6	0	-6.964452	-3.635295	-0.741296
5	1	0	-4.902565	-4.185187	-0.850768
6	1	0	-8.963550	-2.794773	-0.716900
7	6	0	-6.107536	-1.038518	-1.390687
8	6	0	-5.149178	-2.082873	-1.286597
9	6	0	-3.708764	-1.801975	-1.465234
10	7	0	-5.716514	0.264394	-1.647904
11	1	0	-6.471340	0.945707	-1.651606
12	5	0	-4.346555	0.647347	-1.720080

13	6	0	-3.292236	-0.462312	-1.627600
14	6	0	-1.924584	-0.117622	-1.702404
15	7	0	-3.893568	1.991638	-1.882621
16	1	0	-4.534515	2.779182	-1.918440
17	6	0	-1.557471	1.313445	-1.753488
18	6	0	-2.552896	2.323800	-1.840478
19	6	0	-2.166074	3.679194	-1.859377
20	6	0	-0.838612	4.056369	-1.744987
21	6	0	0.155908	3.070107	-1.619194
22	6	0	-0.226093	1.722012	-1.643279
23	1	0	-2.945293	4.442312	-1.939787
24	1	0	-0.567319	5.113987	-1.735992
25	1	0	0.567272	0.981817	-1.525129
26	6	0	-2.727209	-2.806845	-1.437465
27	6	0	-0.970274	-1.145519	-1.678634
28	6	0	-1.380530	-2.471896	-1.558621
29	1	0	0.097874	-0.933060	-1.747284
30	1	0	-0.627373	-3.264386	-1.538203
31	1	0	-2.995167	-3.859044	-1.328670
32	1	0	-7.286780	-4.645653	-0.481741
33	6	0	5.339784	0.780853	-0.139469
34	6	0	6.306881	1.616222	0.512268
35	6	0	4.262312	1.371190	-0.778985
36	6	0	6.137415	3.033879	0.503700
37	6	0	4.023486	2.789054	-0.677384
38	6	0	4.966165	3.591922	-0.072935
39	1	0	4.796598	4.668936	-0.002954
40	6	0	5.343675	-0.703195	0.003063
41	6	0	4.272634	-1.263167	0.652083
42	6	0	6.343926	-1.563749	-0.595939
43	6	0	6.206935	-2.994148	-0.450566
44	6	0	4.068607	-2.697824	0.721284
45	6	0	5.092481	-3.539222	0.195967
46	1	0	4.977181	-4.623608	0.254469
47	6	0	-5.699071	3.303916	0.976309
48	6	0	-7.488694	1.195395	1.197837
49	6	0	-7.956887	2.464725	0.899409
50	6	0	-7.054416	3.530025	0.778860
51	1	0	-5.011262	4.145583	0.877515
52	1	0	-9.027821	2.628598	0.758157
53	6	0	-6.112677	0.954525	1.375710
54	6	0	-5.186897	2.029485	1.283638
55	6	0	-3.739935	1.792601	1.454054
56	7	0	-5.678909	-0.338925	1.608831
57	1	0	-6.410954	-1.045682	1.602553
58	5	0	-4.301630	-0.667137	1.678737
59	6	0	-3.281475	0.466617	1.604907
60	6	0	-1.904470	0.164473	1.684015
61	7	0	-3.800799	-2.011835	1.830835
62	1	0	-4.424914	-2.815838	1.863647
63	6	0	-1.488361	-1.253140	1.738164
64	6	0	-2.474022	-2.299763	1.815283
65	6	0	-2.052963	-3.665998	1.861911
66	6	0	-0.733638	-4.013377	1.789106

67	6	0	0.269623	-2.993340	1.658092
68	6	0	-0.160046	-1.626121	1.653203
69	1	0	-0.433776	-5.062635	1.813307
70	1	0	0.621780	-0.875538	1.526472
71	6	0	-2.788403	2.828517	1.440900
72	6	0	-0.982946	1.219774	1.670347
73	6	0	-1.433406	2.535670	1.560416
74	1	0	0.090910	1.038559	1.738155
75	1	0	-0.704956	3.350390	1.547741
76	1	0	-3.089409	3.872231	1.339798
77	1	0	-8.182349	0.355231	1.289659
78	1	0	-7.411562	4.533202	0.537817
79	6	0	1.550147	3.315892	-1.390700
80	6	0	2.732664	3.227999	-1.115879
81	6	0	1.624095	-3.220516	1.492424
82	6	0	2.826899	-3.100886	1.175889
83	8	0	3.302543	-0.472015	1.191061
84	8	0	3.321625	0.683023	-1.458174
85	6	0	7.427344	-1.050609	-1.330452
86	6	0	8.387258	-1.887861	-1.888285
87	1	0	9.220821	-1.464126	-2.452615
88	6	0	8.280621	-3.286741	-1.721496
89	1	0	9.039396	-3.943973	-2.154316
90	6	0	7.222509	-3.827252	-1.026788
91	1	0	7.130831	-4.910736	-0.910178
92	1	0	7.511588	0.032375	-1.457070
93	6	0	7.107683	3.857972	1.138512
94	6	0	8.192221	3.306922	1.778226
95	1	0	8.931056	3.948845	2.263319
96	6	0	8.342392	1.898586	1.821662
97	1	0	9.194562	1.461500	2.347697
98	6	0	7.423680	1.076012	1.209947
99	1	0	7.546782	-0.008430	1.252713
100	1	0	6.966366	4.942084	1.115566
101	1	0	-2.823394	-4.437432	1.943253
102	1	0	-8.193817	-0.506662	-1.295011
103	6	0	3.526205	-0.127158	2.545932
104	1	0	4.457750	0.459666	2.647035
105	1	0	2.672060	0.484176	2.870104
106	1	0	3.590536	-1.032765	3.175842
107	6	0	3.686328	-0.355712	-2.349742
108	1	0	3.042476	-0.252498	-3.236842
109	1	0	4.744048	-0.263572	-2.648327
110	1	0	3.525656	-1.346486	-1.894984

---



---

Ground to excited state transition electric dipole moments (Au):

state	X	Y	Z	Dip. S.	Osc.
1	4.3798	-0.9970	-1.0429	21.2644	1.6052
2	3.9893	1.0529	0.6679	17.4693	1.5763
3	0.8475	0.3955	-0.1127	0.8874	0.0820

Ground to excited state transition velocity dipole moments (Au):

state	X	Y	Z	Dip. S.	Osc.

1	-0.5054	0.1209	0.1214	0.2847	1.6764
2	-0.5488	-0.1517	-0.0926	0.3328	1.6391
3	-0.1303	-0.0591	0.0159	0.0207	0.0997

Ground to excited state transition magnetic dipole moments (Au):

state	X	Y	Z
1	-0.9220	-2.4504	-3.6228
2	-1.1092	2.0774	4.0951
3	1.0226	-0.2219	0.1561

Ground to excited state transition velocity quadrupole moments (Au):

state	XX	YY	ZZ	XY	XZ	YZ
1	-3.1592	-0.3051	0.1491	1.9471	0.3656	-0.4163
2	-3.1725	-0.3284	0.1310	-1.1596	-0.3399	-0.4276
3	1.4533	0.4871	0.0042	0.5760	0.0869	-0.9475

$\langle 0 | \text{del} | b \rangle * \langle b | \text{rxdel} | 0 \rangle + \langle 0 | \text{del} | b \rangle * \langle b | \text{delr+rdel} | 0 \rangle$

Rotatory Strengths (R) in cgs ( $10^{**-40}$  erg-esu-cm/Gauss)

state	XX	YY	ZZ	R(velocity)	E-M Angle
1	-1697.7670	1.2251	11.2239	-561.7726	96.50
2	-1668.1895	932.1546	288.5620	-149.1576	91.80
3	76.3257	-42.0326	-634.8133	-200.1734	140.57

$1/2[\langle 0 | r | b \rangle * \langle b | \text{rxdel} | 0 \rangle + (\langle 0 | \text{rxdel} | b \rangle * \langle b | r | 0 \rangle)^*]$

Rotatory Strengths (R) in cgs ( $10^{**-40}$  erg-esu-cm/Gauss)

state	XX	YY	ZZ	R(length)
1	2855.6994	-1727.6554	-2671.7481	-514.5680
2	3129.2920	-1546.8341	-1934.2236	-117.2552
3	-612.8631	62.0761	12.4329	-179.4514

---

### Summary of chiroptical properties of (*R*)-1 (M06-2X/def2-SV(P))

---

state	$ \mu_e $ $/10^{-20}$ esu-cm	$ \mu_m $ $/10^{-20}$ erg/Gauss	$\cos\theta$ (E-M Angle)	$g_{\text{lum,calcd.}}$ (4R/(D+G))	$E_{\text{ex}}$ /nm
1	1173	4.145	-0.11320	0.00150	395

---

**Table S2.** Cartesian coordinates (Å) and transition moments of the optimized structure of (*R*)-2 in CH<sub>2</sub>Cl<sub>2</sub> in the lowest-energy excited state (S<sub>1</sub>) calculated at the M06-2X/def2-SV(P) level of theory.

Center Number	Atomic Number	Atomic Type	Coordinates (Angstroms)		
			X	Y	Z
1	6	0	-3.427928	-3.784527	1.983128
2	6	0	-0.601606	-3.936100	1.764994
3	6	0	-1.371110	-5.108495	1.933196
4	6	0	-2.754629	-5.016380	2.037049
5	1	0	-4.514713	-3.778090	2.063264
6	1	0	-0.870600	-6.077476	1.945164
7	6	0	-1.297505	-2.643555	1.781084
8	6	0	-2.726514	-2.571735	1.850930
9	6	0	-3.393816	-1.267780	1.767060
10	7	0	-0.548822	-1.529909	1.690941

11	1	0	0.464757	-1.659541	1.598885
12	5	0	-1.107183	-0.197722	1.719271
13	6	0	-2.618186	-0.081610	1.763197
14	6	0	-3.200579	1.201573	1.707912
15	7	0	-0.319149	0.977516	1.691586
16	1	0	0.695441	0.951936	1.589973
17	6	0	-2.316833	2.382130	1.768274
18	6	0	-0.901512	2.233668	1.783767
19	6	0	-0.077968	3.368002	1.904977
20	6	0	-0.622070	4.637870	1.977673
21	6	0	-2.013116	4.803498	1.932194
22	6	0	-2.833703	3.690558	1.833793
23	1	0	1.006660	3.226722	1.927795
24	1	0	0.036352	5.505610	2.063820
25	1	0	-3.914500	3.838449	1.816783
26	6	0	-4.792411	-1.137973	1.675303
27	6	0	-4.600926	1.290019	1.607913
28	6	0	-5.370317	0.126923	1.585220
29	1	0	-5.105136	2.254419	1.530242
30	1	0	-6.455825	0.209800	1.488036
31	1	0	-5.438666	-2.016760	1.641427
32	1	0	-3.341681	-5.931327	2.150801
33	1	0	-2.452756	5.802066	1.979628
34	6	0	4.011758	-0.809246	-0.183142
35	6	0	4.941904	-1.505370	-1.042078
36	6	0	3.108163	-1.524819	0.556063
37	6	0	4.923436	-2.942055	-1.049723
38	6	0	3.001209	-2.965498	0.475433
39	6	0	3.963693	-3.645613	-0.299677
40	1	0	3.926319	-4.734997	-0.364733
41	6	0	3.941407	0.677385	-0.140524
42	6	0	2.806007	1.305914	-0.613692
43	6	0	4.996741	1.466285	0.425210
44	6	0	4.869565	2.886673	0.467344
45	6	0	2.663728	2.733051	-0.550033
46	6	0	3.687487	3.495428	-0.023926
47	1	0	3.583026	4.581707	0.024346
48	6	0	-4.262810	-3.462764	-1.535470
49	6	0	-1.503075	-3.509743	-1.263620
50	6	0	-2.208057	-4.701540	-1.294616
51	6	0	-3.600768	-4.680836	-1.421458
52	1	0	-5.348630	-3.472461	-1.642522
53	1	0	-1.672183	-5.649339	-1.205307
54	6	0	-2.168430	-2.271374	-1.364401
55	6	0	-3.583338	-2.234316	-1.521510
56	6	0	-4.293384	-0.944406	-1.658805
57	7	0	-1.429926	-1.105149	-1.313803
58	1	0	-0.432382	-1.226839	-1.157327
59	5	0	-2.032390	0.184169	-1.435198
60	6	0	-3.547412	0.254585	-1.625766
61	6	0	-4.162469	1.521225	-1.737863
62	7	0	-1.299463	1.402306	-1.398238
63	1	0	-0.290654	1.418933	-1.232501
64	6	0	-3.321105	2.737157	-1.672919

65	6	0	-1.913725	2.630058	-1.509134
66	6	0	-1.119654	3.811880	-1.451392
67	6	0	-1.716464	5.070134	-1.542013
68	6	0	-3.097111	5.177448	-1.695073
69	6	0	-3.873975	4.025886	-1.758881
70	1	0	-1.087121	5.960548	-1.484709
71	1	0	-4.952304	4.137093	-1.880897
72	6	0	-5.685006	-0.856058	-1.816983
73	6	0	-5.556920	1.571002	-1.895936
74	6	0	-6.295852	0.390995	-1.935379
75	1	0	-6.084931	2.520642	-1.991067
76	1	0	-7.380373	0.444363	-2.060359
77	1	0	-6.310424	-1.749105	-1.850699
78	1	0	-0.414503	-3.511896	-1.150677
79	1	0	-4.169649	-5.612867	-1.436092
80	1	0	-3.568922	6.159275	-1.765013
81	6	0	0.763926	-3.881599	1.498454
82	6	0	1.883959	-3.547967	1.076109
83	6	0	0.283040	3.634718	-1.243887
84	6	0	1.419048	3.287326	-0.982431
85	8	0	1.747857	0.620128	-1.135168
86	8	0	2.236896	-0.868876	1.394493
87	6	0	6.167556	0.873115	0.975411
88	6	0	7.163990	1.652072	1.516851
89	1	0	8.055180	1.178458	1.935146
90	6	0	7.045218	3.064700	1.538453
91	1	0	7.846426	3.670499	1.967585
92	6	0	5.920684	3.665851	1.027704
93	1	0	5.811283	4.753379	1.048092
94	1	0	6.266795	-0.214699	0.963862
95	6	0	5.869379	-3.623924	-1.877221
96	6	0	6.758027	-2.928900	-2.664272
97	1	0	7.469455	-3.471891	-3.291730
98	6	0	6.751321	-1.514335	-2.673951
99	1	0	7.450879	-0.967618	-3.309814
100	6	0	5.856069	-0.824015	-1.874501
101	1	0	5.853746	0.269171	-1.881886
102	1	0	5.864249	-4.717407	-1.879176
103	6	0	1.967345	-0.158451	-2.308056
104	1	0	2.139625	-1.217209	-2.052498
105	1	0	1.062849	-0.066422	-2.929896
106	1	0	2.835241	0.224011	-2.870370
107	6	0	2.721554	-0.756693	2.729639
108	1	0	3.635266	-0.137219	2.749234
109	1	0	1.931317	-0.270978	3.321282
110	1	0	2.936911	-1.755273	3.147544

---

Ground to excited state transition electric dipole moments (Au):

state	X	Y	Z	Dip. S.	Osc.
1	-2.7340	0.8436	0.8726	8.9476	0.6393
2	2.4746	0.6515	0.4818	6.7805	0.5659

3	1.2809	-0.1691	-1.0903	2.8580	0.2523
---	--------	---------	---------	--------	--------

Ground to excited state transition velocity dipole moments (Au):

state	X	Y	Z	Dip. S.	Osc.
1	0.3046	-0.0987	-0.0955	0.1116	0.6942
2	-0.3261	-0.0873	-0.0626	0.1179	0.6276
3	-0.1720	0.0259	0.1472	0.0519	0.2615

Ground to excited state transition magnetic dipole moments (Au):

state	X	Y	Z
1	1.1555	1.5637	3.0616
2	-0.9889	1.0796	2.2918
3	0.1560	-0.6472	-2.4510

Ground to excited state transition velocity quadrupole moments (Au):

state	XX	YY	ZZ	XY	XZ	YZ
1	0.9115	0.3453	-0.0342	-1.1128	-0.1890	0.0965
2	-0.0175	-0.5939	0.1521	-0.7184	0.5597	0.0643
3	-1.6076	0.7210	-0.0065	1.8396	1.1549	-1.0890

$\langle 0 | \text{del} | b \rangle * \langle b | \text{rxdel} | 0 \rangle + \langle 0 | \text{del} | b \rangle * \langle b | \text{delr+rdel} | 0 \rangle$

Rotatory Strengths (R) in cgs ( $10^{**-40}$  erg-esu-cm/Gauss)

state	XX	YY	ZZ	R(velocity)	E-M Angle
1	-1184.4252	-57.3017	616.5571	-208.3900	94.49
2	-406.4936	318.9302	565.7389	159.3918	84.80
3	-365.1711	-1257.9083	-536.7840	-719.9545	134.32

$1/2[\langle 0 | r | b \rangle * \langle b | \text{rxdel} | 0 \rangle + (\langle 0 | \text{rxdel} | b \rangle * \langle b | r | 0 \rangle)^*]$

Rotatory Strengths (R) in cgs ( $10^{**-40}$  erg-esu-cm/Gauss)

state	XX	YY	ZZ	R(length)
1	2233.9461	-932.7952	-1889.1673	-196.0055
2	1730.4895	-497.4240	-780.7647	150.7669
3	-141.2613	-77.3766	-1889.8058	-702.8146

Summary of chiroptical properties of (*R*)-2 (M06-2X/def2-SV(P))

state	$ \mu_e $ $/10^{-20}$ esu-cm	$ \mu_m $ $/10^{-20}$ erg/Gauss	$\cos\theta$ (E-M Angle)	$g_{\text{lum,calcd.}}$ (4R/(D+G))	$E_{\text{ex}}$ /nm
1	761	3.364	-0.07829	0.00135	432

## 5. Cartesian Coordinates

All Cartesian coordinates given below were computed at the r<sup>2</sup>SCAN-3c/def2-mTZVPP level of theory level alongside the continuum solvation model SMD<sup>16</sup> and are given in Å and absolute energies are given in atomic units.

110

	(R) -1 from CENSO, -2804.78378765		
6	6.538833990	0.255254158	-2.705917106
6	7.971682988	-1.587324017	-1.212005082
6	8.642120167	-0.703356444	-2.037179467
6	7.921581439	0.229311724	-2.788697793
1	6.002064761	0.982810653	-3.305709223
1	9.726710253	-0.736143466	-2.095110247
6	6.570608073	-1.562826850	-1.115624606
6	5.820069291	-0.630066392	-1.882632794
6	4.352116257	-0.607159441	-1.805575576
7	5.938328319	-2.458966335	-0.270923695
1	6.560624563	-3.062581672	0.252685073
5	4.524469495	-2.496887684	-0.125862961
6	3.695109582	-1.529251739	-0.955303531
6	2.284200888	-1.557291589	-0.846732554
7	3.836569028	-3.392773146	0.748062830
1	4.320128520	-4.056536463	1.341433935
6	1.662725045	-2.516054383	0.082279982
6	2.462171708	-3.399435954	0.862093216
6	1.848732165	-4.283623934	1.768981452
6	0.481228467	-4.301586119	1.941338414
6	-0.330080879	-3.425881275	1.192515688
6	0.279980395	-2.559585328	0.274180589
1	2.478641271	-4.953656858	2.350071946
1	0.028224393	-4.980731171	2.657119509
1	-0.366927603	-1.890457737	-0.281403917
6	3.568214236	0.293456440	-2.543230584
6	1.536251677	-0.656196849	-1.616554962
6	2.182903584	0.251976446	-2.446580870
1	0.452674330	-0.636536714	-1.574473809
1	1.588284763	0.951362028	-3.029120723
1	4.019245334	1.028938241	-3.200260704
1	8.438084964	0.928558288	-3.439982448
6	-5.617412387	-0.735951878	0.447184956
6	-6.542358167	-0.895737988	1.524472354
6	-4.518239305	-1.575458248	0.370644287
6	-6.309940817	-1.911748491	2.509392210
6	-4.206826948	-2.488515827	1.435804150
6	-5.118913961	-2.665792822	2.459755093
1	-4.899789721	-3.370360115	3.257369445
6	-5.682611454	0.432220029	-0.469129743
6	-4.657545316	1.352878055	-0.377911307
6	-6.692533400	0.608307986	-1.462558118
6	-6.630767378	1.747941158	-2.329166284

6	-4.533620897	2.436590909	-1.310580188
6	-5.534871242	2.633584924	-2.245744956
1	-5.454079042	3.449125618	-2.959349861
6	6.226596736	-0.222684788	2.477107169
6	7.618530113	1.545330702	0.859276052
6	8.310966103	0.636949265	1.638239940
6	7.611091495	-0.258760679	2.451501061
1	5.706767114	-0.927353811	3.117718241
1	9.397047905	0.620158687	1.609616164
6	6.214972465	1.584248598	0.874673911
6	5.485228865	0.688692213	1.703553582
6	4.015706284	0.730062783	1.739350371
7	5.560190006	2.506528175	0.076509552
1	6.167940167	3.095227011	-0.480109754
5	4.142398802	2.609834728	0.043670477
6	3.336260721	1.665818577	0.921986767
6	1.923604611	1.740613488	0.905185403
7	3.431747957	3.562714029	-0.748901775
1	3.899278074	4.225353363	-1.356124173
6	1.277757358	2.700993141	-0.005423208
6	2.055036817	3.592696811	-0.799358589
6	1.414791862	4.503082875	-1.661219200
6	0.043638773	4.519246435	-1.799146573
6	-0.742599600	3.611977168	-1.062194923
6	-0.107877090	2.734442324	-0.171034529
1	-0.429834778	5.212347910	-2.487711472
1	-0.738384620	2.041984167	0.375293094
6	3.252497080	-0.126829149	2.546422812
6	1.196189311	0.878200618	1.736989857
6	1.865933284	-0.037236547	2.540513830
1	0.112116223	0.898250509	1.767637615
1	1.288852053	-0.709293193	3.171344253
1	3.720335421	-0.866992414	3.186603123
1	8.152352894	2.243162535	0.217810577
1	8.145759395	-0.978335307	3.064773681
6	-1.731010729	-3.328244760	1.359311317
6	-2.916894306	-3.064779953	1.424445799
6	-2.138645961	3.468710605	-1.227380099
6	-3.306753651	3.136257402	-1.299270843
8	-3.663930563	1.169151116	0.544439794
8	-3.601848990	-1.553568028	-0.628133446
6	-7.743203636	-0.321893852	-1.641399718
6	-8.707903823	-0.120807433	-2.602417385
1	-9.508757750	-0.845125117	-2.723069542
6	-8.664121027	1.016754772	-3.436335460
1	-9.433261522	1.163335144	-4.189532735
6	-7.644083744	1.928012161	-3.304686220
1	-7.590348837	2.797465804	-3.955464105
1	-7.783527666	-1.201607970	-1.005335088
6	-7.241441916	-2.083364783	3.563797128
6	-8.346047438	-1.272295025	3.668478621
1	-9.052628327	-1.411797518	4.481783379

6	-8.551445509	-0.241517630	2.727551910
1	-9.412690848	0.413511008	2.827387386
6	-7.670134320	-0.054005073	1.686602494
1	-7.840851340	0.748003969	0.975280220
1	-7.055374631	-2.864254808	4.297422572
1	2.027570224	5.187962531	-2.243044910
1	8.522224132	-2.312100268	-0.616010398
6	-3.745458135	2.059164481	1.673999827
1	-2.901514143	1.813607541	2.322278539
1	-3.676146034	3.108536480	1.363072100
1	-4.684358168	1.897723204	2.219184315
6	-4.044407574	-1.434073874	-1.993494641
1	-3.996473116	-0.397559702	-2.341437342
1	-3.354664227	-2.045041385	-2.582880349
1	-5.063287256	-1.818694680	-2.108502374

110

**(R) -2'** from CENSO, -2804.80129876

6	-3.253550044	-5.158399115	-0.152774691
6	-0.551296783	-4.513020708	-0.274575590
6	-0.992467963	-5.770764757	-0.695871434
6	-2.341253424	-6.092798949	-0.624368212
1	-4.301112400	-5.436547422	-0.122126286
1	-0.267565469	-6.480455110	-1.082573697
6	-1.482401801	-3.559425898	0.236799727
6	-2.865225230	-3.879809071	0.278778892
6	-3.846647195	-2.881362550	0.736129826
7	-1.019035889	-2.336360798	0.660445314
1	-0.014045304	-2.202326198	0.578640508
5	-1.895682441	-1.318214913	1.143662630
6	-3.385972630	-1.614551239	1.171212859
6	-4.285262769	-0.610573817	1.607960979
7	-1.460165467	-0.043402413	1.600540153
1	-0.488962149	0.244759934	1.592336378
6	-3.746277919	0.682954527	2.053786009
6	-2.345592829	0.925806721	2.040694937
6	-1.842667299	2.165452153	2.468192272
6	-2.693810554	3.168472345	2.893521212
6	-4.074852353	2.952192048	2.901642853
6	-4.579253166	1.729895072	2.488926425
1	-0.767082839	2.328333023	2.443973830
1	-2.284282662	4.122910536	3.213228101
1	-5.653905478	1.583869070	2.505911051
6	-5.226959369	-3.126189247	0.738004843
6	-5.658678452	-0.894997602	1.595043984
6	-6.106926871	-2.137184363	1.162858139
1	-6.390845809	-0.162782610	1.917204429
1	-7.174561683	-2.341657671	1.156537131
1	-5.634808490	-4.075470226	0.409592672
1	-2.685643900	-7.070742163	-0.945842400
1	-4.752269630	3.735425481	3.228731581
6	4.204750914	-0.730993506	0.076454547

6	5.287501848	-1.078861448	-0.791432209
6	3.133520205	-1.595498964	0.199649701
6	5.246240499	-2.313915713	-1.514211184
6	3.064503955	-2.806780976	-0.566990301
6	4.118434657	-3.149997095	-1.394282720
1	4.070450168	-4.070387242	-1.969375269
6	4.167454223	0.585411033	0.761994975
6	3.207663897	1.511144443	0.401437260
6	5.047339102	0.878208727	1.851100128
6	4.922078627	2.123935279	2.545517497
6	3.040075751	2.732488447	1.135556560
6	3.902724098	3.024241342	2.176696310
1	3.781825687	3.951542745	2.729524381
6	-3.914317276	-1.635247057	-3.306550515
6	-1.207479859	-2.061703520	-2.894777251
6	-1.977456977	-3.052274721	-3.475623733
6	-3.344375164	-2.841597493	-3.679009779
1	-4.975515043	-1.492438858	-3.479766674
1	-1.516504823	-3.992784488	-3.765422396
6	-1.778447436	-0.839036453	-2.506233903
6	-3.162972442	-0.599083825	-2.722198496
6	-3.768848826	0.685630738	-2.339844684
7	-0.975198281	0.119995846	-1.911827178
1	-0.016132126	-0.166676358	-1.756047418
5	-1.478024447	1.390959370	-1.518719726
6	-2.944532775	1.692211265	-1.779132933
6	-3.465835886	2.957019014	-1.411960352
7	-0.691255604	2.397758112	-0.882204610
1	0.284495016	2.254701377	-0.632816075
6	-2.561223726	3.958052092	-0.821164434
6	-1.209063336	3.624910013	-0.543364141
6	-0.372712201	4.566728273	0.128474755
6	-0.863974088	5.832772081	0.459472017
6	-2.172716232	6.172801752	0.143482331
6	-3.000776801	5.245599515	-0.475439457
1	-0.211245234	6.534300313	0.969846909
1	-4.022214970	5.537515628	-0.693060665
6	-5.134075491	0.961097286	-2.507504549
6	-4.835622887	3.192662163	-1.594885411
6	-5.644737786	2.198121418	-2.132947092
1	-5.291124881	4.135579709	-1.313247062
1	-6.706436364	2.392792286	-2.261601669
1	-5.813082338	0.224401272	-2.922472550
1	-0.144878272	-2.219566783	-2.721405737
1	-3.959639418	-3.616067545	-4.127409758
1	-2.554514360	7.158406571	0.390978515
6	0.794454587	-4.107946267	-0.386541312
6	1.881056910	-3.568993826	-0.477588640
6	0.918151923	4.133090672	0.494656990
6	1.942794047	3.551923325	0.798026321
8	2.299800921	1.317285912	-0.600042717
8	2.036122388	-1.350962358	0.971596718

6	6.014836763	-0.049145812	2.307189981
6	6.839712842	0.253480177	3.366702473
1	7.575535510	-0.473321692	3.699546189
6	6.737014191	1.495275945	4.028376184
1	7.397228633	1.720051040	4.861214922
6	5.792760093	2.408673549	3.627514117
1	5.688261248	3.361239326	4.141211118
1	6.101765408	-1.011574611	1.812570010
6	6.319535326	-2.653084662	-2.376158831
6	7.384639547	-1.801375126	-2.540612686
1	8.201224390	-2.068301320	-3.205442288
6	7.411268349	-0.568661460	-1.855069948
1	8.247238146	0.109633192	-2.002167551
6	6.388262472	-0.214467450	-1.004940771
1	6.421077176	0.740510998	-0.489930425
1	6.275402611	-3.597708650	-2.912686151
6	2.784058186	0.979443077	-1.919740188
1	2.794031405	-0.103171489	-2.076286229
1	2.089561901	1.445634025	-2.624101513
1	3.787729427	1.387261349	-2.076690951
6	2.219801416	-1.000839611	2.361567907
1	1.378218209	-1.448202036	2.898237605
1	3.156781259	-1.419175242	2.742781771
1	2.210561466	0.083879636	2.503980480

## References

- 1 F. Zinna, T. Bruhn, C. A. Guido, J. Ahrens, M. Bröring, L. Di Bari, G. Pescitelli, L. Di Bari and G. Pescitelli, *Chem. A Eur. J.*, 2016, **22**, 16089–16098.
- 2 X. Wang, F. Zhang, K. Sebastian Schellhammer, P. Machata, F. Ortmann, G. Cuniberti, Y. Fu, J. Hunger, R. Tang, A. A. Popov, R. Berger, K. Müllen and X. Feng, *J. Am. Chem. Soc.*, 2016, **138**, 11606–11615.
- 3 M. Fingerle, S. Stocker and H. F. Bettinger, *Synth.*, 2019, **51**, 4147–4152.
- 4 M. R. Rapp, W. Leis, F. Zinna, L. Di Bari, T. Arnold, B. Speiser, M. Seitz and H. F. Bettinger, *Chem. A Eur. J.*, 2022, **28**, e202104161.
- 5 Y. Meng, W. T. Slaven IV, D. Wang, T. J. Liu, H. F. Chow and C. J. Li, *Tetrahedron Asymmetry*, 1998, **9**, 3693–3707.
- 6 J. Hua and W. Lin, *Org. Lett.*, 2004, **6**, 861–864.
- 7 Y. Zhao and D. G. Truhlar, *Theor. Chem. Acc.*, 2008, **120**, 215–241.
- 8 F. Neese, *WIREs Comput. Mol. Sci.*, 2012, **2**, 73–78.
- 9 F. Neese, F. Wennmohs, U. Becker and C. Riplinger, *J. Chem. Phys.*, 2020, **152**, 224108.
- 10 F. Neese, *WIREs Comput. Mol. Sci.*, 2022, **12**, e1606.
- 11 S. Grimme, C. Bannwarth and P. Shushkov, *J. Chem. Theory Comput.*, 2017, **13**, 1989–2009.

- 12 F. Weigend and R. Ahlrichs, *Phys. Chem. Chem. Phys.*, 2005, **7**, 3297–3305.
- 13 P. Pracht, F. Bohle and S. Grimme, *Phys. Chem. Chem. Phys.*, 2020, **22**, 7169–7192.
- 14 S. Grimme, *J. Chem. Theory Comput.*, 2019, **15**, 2847–2862.
- 15 S. Grimme, F. Bohle, A. Hansen, P. Pracht, S. Spicher and M. Stahn, *J. Phys. Chem. A*, 2021, **125**, 4039–4054.
- 16 A. V. Marenich, C. J. Cramer and D. G. Truhlar, *J. Phys. Chem. B*, 2009, **113**, 6378–6396.
- 17 H. Kubo, T. Hirose, T. Nakashima, T. Kawai, J. Y. Hasegawa and K. Matsuda, *J. Phys. Chem. Lett.*, 2021, **12**, 686–695.
- 18 F. Furche and R. Ahlrichs, *J. Chem. Phys.*, 2002, **117**, 7433–7447.
- 19 G. Scalmani, M. J. Frisch, B. Mennucci, J. Tomasi, R. Cammi and V. Barone, *J. Chem. Phys.*, 2006, **124**, 094107.
- 20 S. Miertuš, E. Scrocco and J. Tomasi, *Chem. Phys.*, 1981, **55**, 117–129.
- 21 S. Miertuš and J. Tomasi, *Chem. Phys.*, 1982, **65**, 239–245.
- 22 J. L. Pascual-ahuir, E. Silla and I. Tuñon, *J. Comput. Chem.*, 1994, **15**, 1127–1138.
- 23 J. Tomasi, B. Mennucci and R. Cammi, *Chem. Rev.*, 2005, **105**, 2999–3093.
- 24 M. J. Frisch, G. W. Trucks, H. B. Schlegel, G. E. Scuseria, M. A. Robb, J. R. Cheeseman, G. Scalmani, V. Barone, G. a. Petersson, H. Nakatsuji, X. Li, M. Caricato, a. V. Marenich, J. Bloino, B. G. Janesko, R. Gomperts, B. Mennucci, H. P. Hratchian, J. V. Ortiz, a. F. Izmaylov, J. L. Sonnenberg, Williams, F. Ding, F. Lipparini, F. Egidi, J. Goings, B. Peng, A. Petrone, T. Henderson, D. Ranasinghe, V. G. Zakrzewski, J. Gao, N. Rega, G. Zheng, W. Liang, M. Hada, M. Ehara, K. Toyota, R. Fukuda, J. Hasegawa, M. Ishida, T. Nakajima, Y. Honda, O. Kitao, H. Nakai, T. Vreven, K. Throssell, J. a. Montgomery Jr., J. E. Peralta, F. Ogliaro, M. J. Bearpark, J. J. Heyd, E. N. Brothers, K. N. Kudin, V. N. Staroverov, T. a. Keith, R. Kobayashi, J. Normand, K. Raghavachari, a. P. Rendell, J. C. Burant, S. S. Iyengar, J. Tomasi, M. Cossi, J. M. Millam, M. Klene, C. Adamo, R. Cammi, J. W. Ochterski, R. L. Martin, K. Morokuma, O. Farkas, J. B. Foresman and D. J. Fox, 2016.